Published in final edited form as:
J Control Release. 2014 September 28; 0: 381–397. doi:10.1016/j.jconrel.2014.05.059.

Silk-Based Biomaterials for Sustained Drug Delivery

Tuna Yucel[a,b,*], **Michael L. Lovett**[a,b,*], and **David L. Kaplan**[a,†]

[a]Tufts University, Department of Biomedical Engineering, Medford, MA 02155, USA

[b]Ekteino Laboratories, New York, NY 10022, USA

Abstract

Silk presents a rare combination of desirable properties for sustained drug delivery, including aqueous-based purification and processing options without chemical cross-linkers, compatibility with common sterilization methods, controllable and surface-mediated biodegradation into non-inflammatory by-products, biocompatibility, utility in drug stabilization, and robust mechanical properties. A versatile silk-based toolkit is currently available for sustained drug delivery formulations of small molecule through macromolecular drugs, with a promise to mitigate several drawbacks associated with other degradable sustained delivery technologies in the market. Silk-based formulations utilize silk's well-defined nano- through microscale structural hierarchy, stimuli-responsive self-assembly pathways and crystal polymorphism, as well as sequence and genetic modification options towards targeted pharmaceutical outcomes. Furthermore, by manipulating the interactions between silk and drug molecules, near-zero order sustained release may be achieved through diffusion- and degradation-based release mechanisms. Because of these desirable properties, there has been increasing industrial interest in silk-based drug delivery systems currently at various stages of the developmental pipeline from pre-clinical to FDA-approved products. Here, we discuss the unique aspects of silk technology as a sustained drug delivery platform and highlight the current state of the art in silk-based drug delivery. We also offer a potential early development pathway for silk-based sustained delivery products.

Keywords

Silk; Processing; Biocompatibility; Biodegradation; Drugs; Biologics; Mechanisms

[†]**Corresponding author**. Tufts University, Department of Biomedical Engineering, 4 Colby Street, Medford, MA, 02155 USA, Tel: +1 617 627 3251; Fax: +1 617 627 3231.
[*]Both authors contributed equally to this work

Declaration of interest

T.Y., M.L.L. and D.L.K. declare commercial conflicts of interest with Ekteino Laboratories, Inc.

1. Introduction

In sustained drug delivery, the goal is to extend the inter-dose duration for chronic use medications while maintaining nearly constant plasma drug concentrations within the target therapeutic range. Sustained release formulations offer many potential clinical benefits including reduced side effects for therapeutics with low toxic thresholds, improved patient compliance for frequent, difficult, and/or invasive administrations, and decreased costs for third-party payers. The majority of sustained drug delivery formulations on the market or in development are based on synthetic polymers such as polylactide-co-glycolide acid (PLGA) due to their desirable pharmacokinetics and controllable hydrolytic degradation profiles [1]. While they are generally considered safe by the U.S. Food and Drug Administration (FDA), their inherent properties and processing requirements (e.g., acidic polymer degradation products, aqueous/organic solvent interfaces, and processing in organic solvents [2–5]) restrict their use in certain sustained delivery areas, such as protein therapeutics, where these issues may impact product stability. Naturally derived proteins, such as collagen, gelatin, albumin, elastin and milk proteins offer an interesting alternative to PLGA-based systems and are currently under investigation for their potential use in sustained drug delivery [6]. These protein-based materials mitigate some of the drug instability and toxicity concerns related to PLGA but also tend to have relatively rapid dissolution rates in aqueous media, higher batch-to-batch variability, and concerns with sourcing. Thus, any natural protein-based product must offer tunable sustained release kinetics and enhanced product stability, all from a reliably sourced and well-characterized starting material.

To that end, a considerable amount of work has been dedicated to silk protein-based materials for drug delivery applications [7–10]. Silk fibroin offers a unique combination of beneficial properties for drug delivery (Table 1), including controllable biodegradation into noninflammatory by-products [11–15], biocompatibility [12, 15–23], aqueous-based ambient purification [24] and processing options [25], compatibility with sterilization methods [26–29], utility in drug stabilization [30, 31], and robust mechanical properties (Table 1). Furthermore, silk offers a versatile toolkit for various drug delivery applications including not only varied material formats from injectable particles [32–34], bioadhesives [35, 36] and hydrogels [18, 37–39] to reservoirs and scaffold implants [15, 40, 41], but also formulation control points from genetic and sequence modifications [42–44] and bioconjugates [45] to silk material composition and crystallinity [46–48]. By properly matching the physicochemical properties of the target drug with those of the silk format, near-zero order sustained release may be achieved as a function of diffusion- and degradation-based release mechanisms. Because of these desirable properties, industrial interest in silk-based drug delivery systems has grown rapidly, with not only FDA-approved products such as silk sutures (Surusil®, Suru; Sofsilk™, Covidien) and silk scaffolds (Seri® Surgical Scaffold, Allergan), but also amongst companies at various stages of development, such as Ekteino Laboratories (silk-based sustained drug delivery), AMSilk (high performance materials from spider silk), Vaxess (vaccine stabilization), Banner Pharmacaps (silk-based drug delivery platforms), and Immuno-Biological Laboratories (recombinant human proteins made using transgenic silkworms).

In this review, we discuss the unique aspects of silk technology as a sustained drug delivery platform. First, we concentrate on the rare structural features and processing capabilities of silk, highlighting its desirable physicochemical and biological properties. Then, we describe the current state of the art in silk-based drug delivery, and offer a potential early development pathway for a silk-based product.

2. Desirable properties of silk for sustained drug delivery

2.1. Silk structure and self-assembly

In nature, the largest producer of silk is the domestic silkworm *Bombyx mori* (*B. mori*). Silk fibroin is the structural protein component produced in the posterior region of the *B. mori* gland. Due to its well-characterized structural hierarchy and its dominating hydrophobic and block copolymer features, along with its stimuli-responsive self-assembly pathway in aqueous solution, silk fibroin displays unique physicochemical and biological properties desirable for sustained drug delivery applications [49–58] (Figure 1). In essence, silk fibroin is a high molecular weight (≈ 2.3 MDa [59]) protein complex consisting of heavy (Fib-H, $M_{Calculated}$ = 391.6 kDa [60], $M_{Experimental}$ ≈ 350 kDa [57]) and light (Fib-L, M_C = 27.7 kDa [60], M_E = 26 kDa [56]) chains held together with a disulfide bond at the C-terminus [55], physically encapsulating a glycoprotein (Fibrohexamerin or p25, M_C = 25.2 kDa [60]) at a molar ratio of 6:6:1 (Fib-H, Fib-L, p25) [50]. The fibroin heavy chain is the major structural component of the protein complex and is essentially an amphiphilic, alternating block copolymer. This copolymer consists of 12 long hydrophobic “crystallizable” domains and 11 almost identical, less repetitive and more hydrophilic “amorphous” domains, with hydrophilic C- and N-terminal domains all contributing to give the molecule an overall anionic ($pI_{fibroin}$≈4) character in neutral solution. The crystallizable domains provide a major control point for silk formulations, primarily consisting of 66-residue sub-domains, rich in a low-complexity, dipeptide motif of GX (G: Glycine and over 90% of X residues are either alanine, serine, tyrosine or valine in decreasing frequency) and GAAS tetrapeptides. By manipulating the crystal form and content of these domains, the physical properties of a silk-based formulation may be tuned to achieve the desired release kinetics and biodegradation profile.

In aqueous solution, this unique crystallizable sub-domain sequence forms β-strands and 3-strand β-sheetsextending over 20 nm and stabilized by inter-strand hydrogen bonding [58] (Figure 1).. Intramolecular fibroin self-assembly then proceeds by lateral and facial packing of β-sheets via folding around amorphous domains, leading to strong physical interactions such as dense hydrogen bonding and increased hydrophobic interactions. These large, hydrophobic domains are responsible for the robust mechanical properties of silk fibroin that also translate into desirable characteristics for sustained delivery, such as slow biodegradation rates in the absence of chemical crosslinking. Subsequent intermolecular fibroin heavy chain self-assembly results in the formation of micellar structures where the hydrophobic crystallizable domains are encapsulated inside a hydrophilic shell consisting of the “amorphous” domains and C- and N-terminal domains. The morphology of these nano-micelles is essentially spherical due to the relatively small surface area of the hydrophilic

shell to the overall volume of fibroin heavy chain molecules. The manipulation of the self-assembly of these nano-micelles offers another control point for formulation development.

Intermicellar self-assembly is largely controllable and is strongly stimuli responsive in aqueous solution without the use of harsh chemicals, an important distinction from synthetic polymers. In unperturbed aqueous conditions similar to that in the *B. mori* silk glands, fibroin nano-micelles can self-assemble into spherical microglobular superstructures enabling high aqueous solubility of hydrophobic domains via a hydrophilic shell and interspersed hydrophobic-hydrophilic core structures [51] (Figure 1). With external stimuli, such as changes in solution conditions (e.g., fibroin concentration, pH, ionic strength, temperature), protonation or charge screening of hydrophilic domains leads to essentially permanent, physical intermicellar and interglobular crosslinks, and an overall increase in β-sheet content and formation of silk networks [51]. β-sheet crosslink formation can also be triggered by application of mechanical (e.g., shear) [38, 39] or electromagnetic fields [36, 61], presumably due to chain extension and alignment of fibroin micelles and globules, and resulting enhanced physical permanent crosslinking. The stimuli-responsiveness of the silk self-assembly pathway enables the control of effective correlation lengths in the network and facilitates diffusion-controlled release of drug molecules varying in size from small molecules to protein drugs [7–10]. This is all achieved without toxic organic solvents or cross-linkers, thus preserving the stability of any potential protein therapeutic.

As a consequence of these stimuli-responsive self assembly mechanisms, the silk fibroin heavy chain displays crystalline polymorphism with predominantly three crystal forms, silk *I*, *II* and *III* [53, 62]. Silk *I* is the meta-stable, pre-spinning crystal form of silk fibroin in the middle region of the silk gland, primarily consisting of intra- and intermolecular bonding of a repeated type II, β-turn structure [62], and possibly helical structural elements forming a less extended chain confirmation than silk *II* [63]. Silk *II* is the crystal form of the spun silk fibroin fiber, mainly consisting of antiparallel β-sheets [53] with distorted β-sheets and distorted β-turns [62], while silk *III* is a 3-fold extended helix that forms at air-water interfaces [64]. High-order conformation of aqueous regenerated fibroin solutions and fibroin material formats relevant to sustained drug delivery generally contain a mixture of β-sheets, β-turns, helices and random coils. The structural differences in crystallizable and amorphous domains due to crystal polymorphism can result in differences in enzymatic biodegradation rates. Therefore, controlling the overall supramolecular structure is critical to fine tune silk biodegradation, especially when targeting biodegradation-controlled release.

Additional versatility of the silk platform for sustained drug delivery stems from possible chemical modifications, utilizing the reactive residues in silk sequence as reviewed elsewhere [42]. A number of chemical modification approaches, including coupling, side chain modifications and grafting, together with various functional groups and biomacromolecules covalently fused to silk are summarized in Figure 2. Overall, by systematically controlling fibroin primary structure, self-assembly kinetics in aqueous solution, the crystal polymorphism, and the resulting physicochemical properties of silk-based formulations in solution through the solid state can be tuned to achieve a desired pharmacological outcome.

2.2. Aqueous silk fibroin purification

The main goal in silk fibroin purification is to remove the surface coating layer of *B. mori* silk fibers, eliminating potential immunogenic proteins or glycoproteins, as well as possible contamination on the fiber surface [16, 65, 66].

Sericin proteins are key impurities in fibroin purification as they may trigger an immunogenic response *in vivo*. Sericin proteins are secreted in the middle region of the silk gland of *B. mori* and form an adhesive coating around fibroin. They constitute the majority of the native *B. mori* fiber surface layer and up to 30% of the total fiber mass. The main components of sericin proteins are those produced in the anterior (Ser-A, $M_E \approx 250$ kDa), middle (Ser-M, $M_E \approx 450$ kDa), and posterior (Ser-P, $M_E \approx 150$ kDa) regions of the middle silk gland [67], with a total of 5 to ≥12 proteins, possibly including minor sericin components, fragments of major sericin components, or non-silk related *B. mori* polypeptides/glycoproteins, also being identified as sericins [68, 69]. In contrast to fibroin, sericin protein sequences generally contain a higher density of serine and a lower density of glycine residues, as well as a higher density of polar and/or charged groups (such as those in aspartic acid/asparagine and less commonly glutamic acid/glutamine side chains). This results in the overall more hydrophilic and ionic nature of sericin proteins in comparison to fibroin [67, 68].

These differences in overall charge and hydrophobicity of fibroin and sericin proteins present several options for aqueous-based fibroin purification (degumming or desericinization). For example, selective dissolution/hydrolysis of sericins can be conducted at temperatures between ambient to 100°C, in alkali (e.g., sodium carbonate), acids (e.g. citric acid), or high concentration denaturant solutions (e.g. urea), and/or proteases [52]. The most commonly used degumming method in silk fibroin-based sustained delivery literature is alkali-heat degumming (Figure 3). This process involves boiling silkworm silk cocoons in an aqueous, 0.02 M Na_2CO_3 solution and results in an essentially instantaneous (≈ 5 min) dissolution and partial hydrolysis of sericin proteins as well as a degumming time-dependent, partial hydrolysis of fibroin for a controllable molecular weight distribution [24]. Once purified, fibroin can be dissolved in a number of aqueous, chaotropic high concentration salts (e.g., ≥9 M LiBr, ≥50°C or ≥10 M LiSCN, ≥25°C) or ternary systems containing alcohols (e.g., $CaCl_2$–water-ethanol, ≥70°C). Subsequent desalting of high-salt fibroin solutions is generally carried out by dialysis to obtain an aqueous regenerated fibroin solution, though chromatographic desalting protocols have also been proposed [70].

From a physical stability viewpoint, it should be noted that in aqueous solution, fibroin molecules gradually self-assemble into hydrogel networks rich in silk *II*, β-sheet content in an external stimuli-responsive manner [39]. In ambient, neutral solution conditions and without perturbations, fibroin self-assembly and hydrogelation kinetics are rather slow, providing a controllable timeframe for sustained delivery formulation processing. For example, complete hydrogelation duration of alkali-heat purified fibroin at 2–8°C can be tuned between less than 24 hours to over 30 days, simply by varying the fibroin concentration. Furthermore, the physical stability of aqueous fibroin solutions, i.e., the kinetics of fibroin self-assembly and hydrogelation, may depend on fibroin molecular

weight distribution, storage conditions (e.g., solution ionic strength, pH, and temperature) [37], as well as the presence of mechanical [38, 39] or electromagnetic stimuli [35, 36].

The resulting aqueous fibroin solution is typically used as the starting material for processing into materials suitable for drug delivery such as injectable nano/microspheres [32, 33, 71], hydrogels [17, 18, 38, 39] and bioadhesives [35, 36], and implantable scaffolds [15], films, tubes [72] and rods, and transdermal microneedles [73] as reviewed elsewhere [25] (Figure 3).

2.3. Compatibility of silk with common sterilization methods

To eliminate sources of bacterial or viral contamination, sterilization is a critical step in the manufacture of sustained delivery products. However, several common sterilization methods are not compatible with most biodegradable synthetic polymers (e.g., PLGA) or protein-based (e.g., collagen) matrices, primarily due to their low thermal stability and hydrolytic degradation mechanisms [74, 75]. For example, high temperature methods including autoclaving (high steam pressure at 120–135°C) or dry heat sterilization (160–190°C) result in PLGA deformation and degradation, or melting and softening, respectively [74]. Similarly, collagen scaffolds undergo denaturation with autoclaving, and partial denaturation and cross-linking with dry heat sterilization [75]. Physical sterilization methods, such as gamma or beta irradiation could also result in instability and deterioration of PLGA, and cross-linking and/or chain scission of both PLGA and collagen-based matrices [74, 75]. Ethylene oxide terminal sterilization may be suitable for several synthetic polymers and biopolymers, but this process is lengthy and produces toxic residues. On the other hand, disinfection in 70% aqueous ethanol generally does not adequately eliminate hydrophilic viruses and bacterial spores [76]. These limitations associated with sterilization of the polymeric matrix material may create significant hurdles for a pharmaceutical product, including increased manufacturing costs.

Silk-based biomaterials are generally compatible with most common sterilization methods, presumably due to their extraordinary mechanical properties and high thermal stability (glass transition temperature, $T_g \approx$ 190–200°C; decomposition temperature, $T_d \approx$ 220–300°C for side chains, and ≥300°C for the peptide backbone [27]). For example, self-assembled silk fibers consisting of recombinant spider silk analogs retained their predominantly β-sheet structure, nano-scale morphology, and mechanical properties (tensile modulus) after autoclaving, with no signs of hydrolysis [28]. Similarly, the bulk morphology, topography, crystallinity and cytocompatibility of porous silk fibroin scaffolds were minimally affected by common sterilization methods, including autoclaving (121°C, high pressure steam, 15 min), dry heat (180°C, 30 min) ethylene oxide (55°C, 4 h) or exposure to disinfecting agents (70% aqueous ethanol or an antibiotic-antimycotic solution) [77]. Generally, an increase in the stiffness and strength values of silk fibroin scaffolds were observed in compression due to autoclave sterilization [27, 77]. In addition, no detrimental effects of autoclaving were observed on the gross morphology, micro-scale porosity, or mechanical properties of the silk fibroin scaffolds [27]. A thorough physicochemical characterization of possible effects of autoclaving on silk fibroin scaffold structure indicated a slight increase in silk *II*, β-sheet content and crystal size, an overall reduction in

amorphous domain mobility, and higher thermal stability for autoclaved scaffolds compared to non-sterile scaffolds. It was proposed that the changes in supramolecular organization in amorphous domains induced by autoclave sterilization could slow down protease diffusion rates in the silk fibroin matrix and/or hinder enzyme adhesion, effectively reducing enzymatic degradation rates. For sterilization of regenerated silk fibroin solutions and hydrogels, gamma irradiation induced random coil to silk *II*, beta-sheet transition in solution state and reduced the silk fibroin hydrogelation duration, while autoclaving led to less significant molecular conformational changes and slower hydrogelation kinetics than those after gamma irradiation [29]. Neither solution sterilization method had a detectable effect on the final molecular conformation of self-assembled silk fibroin hydrogels, which was rich in silk *II*, β-sheet content. In a thin film format, gamma-irradiation (in air or nitrogen) did not significantly alter the optical or tensile properties of silk fibroin, or adhesion of cells to the silk fibroin film [26]. On the other hand, autoclaving resulted in an increase in silk fibroin film tensile modulus and strength, in a similar fashion to the effect of autoclaving on the mechanical properties of silk fibroin scaffolds [27, 77]. Overall, the potential effects of the sterilization protocol on silk fibroin final material properties and subsequent pharmacological performance should be considered when identifying suitable sterilization methods. From a manufacturing perspective, the general suitability of common sterilization treatments for silk-based biomaterials renders them a desirable sustained drug delivery matrix.

2.4. Silk biocompatibility

Cytocompatibility and low inflammatory potential of silk—The majority of reports over the past 15 years suggest a desirable biocompatibility profile for alkali-heat purified silk fibroin-based materials due to their cytocompatibility and relatively lower or similar immunogenic potential compared to other common degradable polymers, such as collagen and PLGA. For example, *in vitro* cultures of various cell types, including fibroblasts, keratinocytes, hepatocytes, osteoblasts, epithelial, endothelial, glial, and mesenchymal stem cells (MSCs) indicated desirable cytocompatibility profiles for various silk fibroin formats (see for example [78–80]). The inflammatory potential of silk fibroin and fibroin-RGD films cast from hexafluoroisopropanol (HFIP) solution and treated with methanol to enhance silk *II*, β-sheet crystallinity was investigated using human mesenchymal stem cells (hMSCs) [20]. Transient pro-inflammatory (IL-1β) and inflammatory (COX-2) gene expression in response to stimulation with fibroin films was at similar levels to those for collagen or PLA polymer matrices. Furthermore, higher cell proliferation rates were observed for fibroin films as compared to collagen or PLA, highlighting the relatively low immunogenic potential and high cytocompatibility of silk fibroin. Different components of *B. mori* silk were isolated to determine their individual inflammatory potential including (1) *B. mori* silk fibers including sericin-rich surface coating layer, (2) alkali-heat regenerated fibroin fibers, (3) alkali-heat degumming supernatant rich in sericins, (4) regenerated fibroin fibers incubated in the alkali-heat degumming supernatant, and (5) insoluble fibroin particles obtained by chymotrypsin proteolysis of degummed fibroin [21]. The results indicated that stimulation of macrophages with none of the individual silkworm silk components produced elevated levels of pro-inflammatory TNF either in short (1-day) or long-term (7-day) cultures. Further studies investigated possible *in vitro* complement activation by silk fibroin

films (prepared by casting a film of alkali-heat regenerated fibroin solution in LiBr, followed by methanol treatment to induce silk *II*, β-sheet structure) [22]. The silk fibroin films interacted with the humoral inflammatory system in a similar manner as the synthetic polymers, such as polystyrene and poly(2-hydroxyethylmethacrylate) films. Specifically, C3 complement bound strongly to silk fibroin films, presumably due to the nano-scale heterogeneity of silk fibroin surface crystallinity, but without C3 complement activation. Silk fibroin also induced a lower degree of activation and adhesion of immune-competent peripheral blood mononuclear cells (PBMCs) after treatment with plasma proteins as compared to synthetic model polymers.

Biocompatibility of silk implants—Long-term, *in vivo* biocompatibility of model silk fibroin-based systems, including fibroin films and porous scaffolds were investigated in small animal models (Table 2). For example, silk fibroin and fibroin-RGD films seeded with autologous rat mesenchymal stem cells and implanted intramuscularly in Lewis rats demonstrated low inflammatory potential [20]. Histological and immunohistochemical evaluation of the silk explants 6 weeks post-implantation revealed the presence of circumferentially oriented fibroblasts, few blood vessels, macrophages at the implant-host interface, and the absence of giant cells. In comparison to collagen or PLA films, the inflammatory tissue reaction was less pronounced around the fibroin films. In another study, porous, 3D fibroin scaffolds prepared from aqueous or organic solvents at different fibroin concentrations and pore size distribution and pore inter-connectivity were implanted subcutaneously or intramuscularly in nude or Lewis rats [15]. Gross observations, histological and immunohistochemical evaluations, and real time-PCR analyses were conducted at 2, 8, 26, and 52 weeks to investigate acute and long-term immunogenic potential and biodegradation of porous silk fibroin scaffolds. All scaffolds were well tolerated throughout the study with no reported abnormalities. Early responses to both aqueous-based and organic solvent-based fibroin scaffolds were similar; macrophages and giant cells were observed at the administration site after 2 and 8 weeks, respectively resulting in gradual enzymatic biodegradation of silk fibroin scaffolds. Inflammatory gene (IL-4, IL-13, IL-6, TNF-α, and IFN-γ) expression levels generally remained low (and even lower for aqueous-based scaffolds than that for organic solvent-based scaffolds) and local throughout the study with only a slight, transient increase in IFN-γ levels between 2 and 8 weeks. Overall immune response to fibroin scaffolds was described as low to mild, and local and transient, consistent with previous biocompatibility data on fibroin scaffolds and films [20, 81, 82].

Silk injectable hydrogels and micro-gel suspensions—In addition to implantable systems, the biocompatibility of injectable fibroin systems such as hydrogels and micro-gels has also been investigated (Table 2). As an example, the biocompatibility of acidic fibroin hydrogels (2 wt% fibroin, pH < 3.8) was studied in a rabbit critical sized distal femur defect model over 12 weeks and compared to that of PLGA [18]. Bone remodeling was quantified using trabecular bone volume, thickness, number, and separation, and rates of mineral deposition and bone formation. Silk fibroin hydrogels did not elicit a tissue inflammatory reaction and promoted bone remodeling and maturation. Interestingly, regrown bone of fibroin hydrogel treated defects were more similar to native bone than that for PLGA-treated

defects, demonstrating a good biocompatibility profile for acidic fibroin hydrogels in rabbits and their potential in promoting bone remodeling. Similarly, biocompatibility of ethanol-induced, fibroin-based hydrogels was assessed *in vivo* [17]. Fibroin hydrogels and fibroin hydrogels covalently functionalized with a 23-residue peptide containing a cell-binding sequence (fibroin-23RGD) were subcutaneously implanted in male Lewis rats in a 57-day study. All fibroin hydrogels were completely penetrated with host tissue within 57 days, with minimal visible residual material. Histological examination indicated a low-grade but persistent, fibrotic type inflammatory response to fibroin hydrogels and a less robust inflammatory response to fibroin-23RGD hydrogels, indicating that the RGD functionalization could improve biocompatibility through enhanced cell binding and permeability in fibroin hydrogels. This approach was further validated in intradermal injections of fibroin-23RGD hydrogel particle (or microgel) suspensions in comparison to commercial, collagen-based products, such as Zyplast™ (Allergan, CA) and Hylaform™ (Allergan, CA) using a Hartley guinea pig model over 92 days. For all groups, 75% of administration sites had residual test material at termination, indicating comparable long-term, *in vivo* biodegradation rates for fibroin and chemically cross-linked, collagen-based products. Overall, fibroin-23RGD hydrogel was found to be biocompatible, exhibiting similar chronic cellular responses to that for collagen-based products, typically a mild fibrotic reaction with populations of fibroblasts, lymphocytes, macrophages, multi-nucleated giant cells and eosinophils, with abundant deposition of collagen in and around the implant site and no ulcerations.

Biological testing of an FDA-approved silk-based product—While comparison data between silk and other relevant polymer systems is encouraging, general preclinical biological testing of a candidate biodegradable polymeric delivery vehicle may require a more comprehensive series of toxicity assays. These may include cytotoxicity, intradermal and systemic injections, pyrogenicity testing, allergic sensitization, biodegradation, and biocompatibility assays to demonstrate safety in small and large animal models. One silk fibroin-based product that has passed regulatory scrutiny, Seri® Surgical Scaffold (Allergan, MA), is a resorbable matrix of fibroin yarns functionalized with RGD cell-binding domains that is currently approved by the FDA for anterior cruciate ligament repair. Though the FDA may regulate fibroin-based drug delivery systems differently (e.g., drug vs. device), the thorough pre-clinical biological testing conducted on Seri® Surgical Scaffold may be relevant to the development of potential fibroin-based drug products. In terms of biocompatibility, Seri® Surgical Scaffold passed all ISO standard biocompatibility testing, demonstrating non-toxicity, non-pyrogenicity, and non-allergenicity, and overall biocompatibility of the device [12]. Furthermore, Seri® Surgical Scaffold demonstrated greater cellular infiltration than silk sutures in an intramuscular rat model over 30 days, with a fibroin biodegradation mechanism involving epithelioid macrophages associated with granulomatous inflammatory response within the yarns, through secretion of proteases or possible engulfing of fibroin yarns by macrophages. In terms of immunogenicity, total average plasma IgE concentration was essentially constant at baseline levels for 6 months following subcutaneous implantation of Seri® Surgical Scaffold in rats, indicating the absence of a hypersensitivity reaction and low immune response. Safety of Seri® Surgical Scaffold was also demonstrated in a large animal (goat knee) model, with no signs of acute

inflammation, swelling, or scar formation, and active bone remodeling and joint stability over 12 months. Conversely, a positive immunogenic control containing silk scaffold processing impurities showed deleterious responses, such as synovitis and extensive inflammation within the joint.

Common silk processing impurities and contaminants—As reports on the biocompatibility and low inflammatory potential of silk fibroin have multiplied, the majority of early reports on the immunogenic responses to native, virgin silk fibers may be attributed to impurities [66] and/or contaminants on native silkworm silk fiber surface or in the production waste. For silk fiber surface contaminants, studies on the possible immunogenic potential of the sericin-rich, alkali-heat degumming supernatant of *B. mori* fibers showed insignificant macrophage activation [21] and low-level activation of pro-inflammatory and inflammatory mediators [83, 84], generally insufficient to cause inflammatory response or prevent cellular proliferation. Furthermore, *B. mori* silk degumming supernatants containing predominantly partially hydrolyzed (for alkali-heat, acid-heat, heat-pressure degumming) or native sericins (urea degumming) were not toxic to mouse fibroblast cells at concentrations below 40 ug/ml, while cell viability and collagen production at higher concentrations depended on the degree of sericin hydrolysis (e.g., changes in molecular weight, overall surface charge and aggregation state, and amino acid composition).

In addition to sericin impurities, native *B. mori* silk fibers may also contain potentially immunogenic impurities of non-silk origin, such as silkworm excretory products or dust [85]. These contaminants are the result of improper storage or handling and/or processing additives depending on silk sourcing [86]. Clearly, this may lead to differences in the impurity and contaminant profile of material obtained in different research labs due to potential differences in sourcing, storage and handling protocols during purification and processing. Therefore, thorough physicochemical and biological characterization and documentation of identity and purity of test articles is critical to address potential effects of impurities, additives and/or contaminants on the immunogenic potential.

To provide an unbiased comparison of the relative immunogenic potential of different polymer systems, processing should be conducted in a similar lab environment and ideally at a similar scale, with known identity and purity profiles. One comparison of the potential innate and adaptive immune responses to fibroin films and scaffolds, sericin films, and a commercial collagen-based sponge (Ultrafoam™) indicated a decreasing order of monocyte activation (innate response) from bacterial LPS (positive control) > sericin films > fibroin scaffolds > fibroin films > Ultrafoam™, with no adaptive response detected in any of the groups [87]. Despite this result, no information on the quantification of purity and/or impurity or contamination profile for either of the fibroin test articles was provided to ensure their successful sterilization or decontamination (e.g., depyrogenation). On the other hand, one would expect such characterization, documentation and process controls to be in place for the commercial product comparator used in this study. In this sense, this study does not provide an unbiased comparison between immunogenic potential of different proteins, as the test articles were not prepared under identical or similar conditions and process controls. Furthermore, all of the fibroin materials used in the biocompatibility assays reportedly had similar mass and specific surface area values due to the possible dependence of

immunogenic potential on these parameters, while the specific surface area of the collagen-based product was not reported. To investigate a possible link between monocyte activation by fibroin test articles and their potential pyrogenic contamination, the authors added 10 μg/ml Polymyxin B (PMB, a cationic peptide antibiotic that blocks biological effects of pyrogens through binding to their toxic, anionic lipid A components), similar to a previous report [21]. This treatment inhibited activation in the bacterial LPS positive control group, but not that in the fibroin scaffold group, a result that the authors attributed to a monocyte activation pathway for fibroin scaffolds that does not involve potential pyrogenic contamination. It should be noted, however, that PMB could also bind to anionic fibroin scaffold formats due to potentially attractive electrostatic and hydrophobic interactions, decreasing the effective PMB concentration in culture. Furthermore, no data was provided on the possible effects of PMB addition on monocyte response to fibroin films, rendering it difficult to draw any conclusions regarding the innate response to fibroin test articles in this report.

2.5. Silk biodegradation

The unique physicochemistry of silk, including a predominantly hydrophobic structure, strong intramolecular and intermolecular physical interactions, and crystal polymorphism enable tunable and slow silk fibroin biodegradation kinetics in the absence of potentially toxic chemical crosslinkers. Fibroin hydrolysis is predominantly attributed to the action of proteolytic enzymes naturally secreted in the body, including part of the foreign body response cascade [12, 15]. Several potential proteolytic cleavage sites exist in both the amorphous and crystalline domains of fibroin [13], leading to gradual fibroin biodegradation into soluble amino acids and peptide fragments [88] through a proteolysis pathway that may involve non-toxic, supramolecular intermediates [89] and/or tightly-packed aggregates [14]. Fibroin biodegradation time, defined as the time to complete loss of structural integrity and loss of mass of the test article *in vivo* can be fine-tuned per application from <3 months for injectable sonicated hydrogels containing ≤2 wt% silk fibroin in a rat femoral defect model [11], to <6 months to over 12 months depending on fibroin concentration and pore size distribution and connectivity for porous scaffolds with ≤10 wt% silk fibroin in a subcutaneous rat model [15], or an estimated 18–36 months for hydrophilic silk fibroin yarns in a goat knee model [12], covering a desirable timeframe for long-term, sustained delivery applications (Table 2).

Accelerated biodegradation models have been developed *in vitro* to study the critical physicochemical parameters controlling silk fibroin biodegradation. Protease XIV, a mixture of serine proteases ranging in apparent molecular weight from 16 to 27 kDa is commonly used for accelerated *in vitro* silk fibroin degradation studies, mainly due to its low cleavage site selectivity and resulting high *in vitro* silk fibroin degradation rates. For example, protease XIV-mediated degradation of fibroin yarns led to a predictable, gradual reduction in molecular mass of fibroin heavy and light chains, and overall size and mass, and deterioration of mechanical properties [90]. In terms of controlling the rates of silk fibroin degradation, high-order structural aspects of fibroin formats such as the total silk crystal content (e.g., *silk I* and *silk II*), relative fraction of each crystal polymorph [47], and the degree of crystal order (relative concentration of intramolecular to intermolecular *silk II*)

[14] may play an important role. For example, silk fibroin films rich in *silk I*, helical content degraded at significantly faster rates *in vitro* compared to films rich in *silk II*, β-sheet crystal content [47]. Furthermore, *in vitro* enzymatic degradation rates for wet-milled, spray-dried silk fibroin microparticles (<10 μm size) was approximately three times faster than that for silk fibroin fibers at a similar overall crystal content, presumably due to a relative reduction in intermolecular *silk II*, β-sheet content and high specific area (surface area/volume) values for microparticles [14]. In addition to silk crystal structure, molecular weight also appears to influence silk fibroin biodegradation. For example, faster silk *in vitro* enzymatic degradation rates induced by increasing the alkali-heat degumming time were attributed to the reduction in the average molecular weight [91]. This hypothesis could be further supported by the quantitation of fibroin molecular weight distribution as well as the isolation of possible effects of average molecular weight and polydispersity and the possible changes in fibroin primary structure with varied durations of alkali-heat degumming. The biodegradation rates are further impacted by silk concentration as increasing the silk fibroin concentration reduced *in vitro* enzymatic degradation rates for sonication-induced hydrogels [38]. This mirrors the effect of fibroin protein concentration on the *in vivo* biodegradation rates observed for porous fibroin scaffolds [15]. Overall, silk fibroin proteolysis can be tuned through silk fibroin purification and processing, with resulting differences in structure and morphology controlling the biodegradation rates for any given silk format.

Biodegradation heterogeneity vs. drug stability and pharmacokinetics—The enzymatic nature of silk biodegradation presents additional potential advantages in sustained delivery of low stability drugs and/or applications requiring zero-order pharmacokinetics. Generally, macro-scale homogeneity of a polymer biodegradation process may depend on the relative rate of diffusion (D) of the hydrolyzing agent in the polymer matrix to the rate of polymer hydrolysis (H). In case of a hydrophilic, highly porous network, D >> H would lead to homogenous or bulk biodegradation, while H >> D for a non-porous, hydrophobic system would lead to heterogeneous biodegradation confined predominantly to the surface of the matrix. For example, bulk hydrolysis commonly observed for PLGA polymers results in prolonged exposure of the therapeutic compound to undesirable acidic PLGA polymer hydrolysis products, while the surface erosion commonly observed for silk fibroin could enable diffusion of biodegradation products away from the active site, reducing the loss in drug stability, activity and/or safety. For example, *in vitro* proteolytic degradation of fibroin yarns was essentially confined to the yarn surface leading to a reduction in fiber diameter and visible surface particulate debris that correlated well with a reduction of overall mass, indicating the heterogeneous, surface mediated biodegradation of silk fibroin [90]. From a pharmacokinetic perspective, generally heterogeneous biodegradation characteristics of predominantly hydrophobic, silk-based dosage forms may also provide zero-order sustained release of drugs as discussed further in section 3.2. The biodegradation rates may be further impacted by the cellular interpenetration and enzymatic diffusion rates in silk fibroin networks. For example, cellular and protease diffusion rates may be higher for self-assembled, highly hydrated, low fibroin concentration hydrogel networks, or porous fibroin scaffolds [15] as compared to high solid density, hydrophobic fibroin yarns or films, potentially leading to more homogeneous silk fibroin matrix biodegradation. Even though determining specific silk fibroin biodegradation pathways is important for fibroin-based

product development, one would not expect a correlation between the macro-scale homogeneity of fibroin biodegradation and the suitability of fibroin formulations for a specific drug delivery application since the eventual biodegradation products of silk fibroin are essentially neutral amino acids, not acidic byproducts as with PLGA hydrolysis.

2.6. Which silk to use?

Generally, formulation scientists considering silk protein-based vehicles for sustained delivery have two options: naturally-derived, regenerated silk fibroin or genetically engineered, synthetic silk analogs. Silk sourcing may be one of the most critical parameters for sustained delivery applications, with potential effects on the identity, purity, and physicochemical characteristics of a potential silk product and subsequently its biological response and the pharmacological outcome. Silk fibroin is available in large quantities in Nature, and can be readily purified in aqueous-based, non-toxic solvents with relatively low energy input and potentially low manufacture costs. Silk fibroin structure, physicochemical properties and long-term biological response can be controlled through fibroin purification, its stimuli-responsive self-assembly and processing, providing a viable platform for sustained delivery applications. On the other hand, synthetic silk analogs may provide higher levels of control over silk molecular structure and purity as compared to silk fibroin, while potentially requiring higher cost of goods. Therefore, the utility of synthetic silk analogs in sustained delivery may depend on whether they can provide more reproducible and/or desirable pharmaceutical outcomes than those achievable using naturally derived silk fibroin.

3. Current state of the art in sustained drug delivery using silk

3.1. Drug delivery applications of silk technology

Silk has been utilized as a vehicle to deliver a wide range of bioactive molecules including genes [43, 92–95], small molecules [34, 96–99], and biological drugs [33, 100–103]. For each class of molecules, various silk technologies (Figure 3) have been applied for the delivery and controlled release of therapeutic drugs [7–10]. The combination of silk material platforms, processing conditions, and drug compounds used in prior work, and ultimately drug release kinetics and mechanisms, are instructive for any future drug delivery application.

Gene delivery—For gene delivery, recombinant silk analogs or silk-like polymers are commonly used to deliver plasmid DNA or adenoviral vectors (Table 3). These silk-based block copolymers are typically utilized for this application due to their ability to be functionalized, an important advantage over other gene delivery vehicles such as liposomes and synthetic polymers [8]. As an example, genetic engineering approaches have been used to form block copolymers of spider silk consensus repeats and poly(L-lysine) domains to form ionic complexes that deliver plasmid DNA [43, 104]. These gene carriers may then be functionalized with cell penetrating and cell membrane destabilizing peptides to enhance transfection efficiency [105] or bioengineered as complexes to home specifically to targets such as tumor cells using tumor-homing peptide [95]. Additional functionality may also be gained by producing silk variants such as silk-elastin-like polymers to achieve fine control

over the material properties and biodegradation rates of a given formulation. As an example, these polymers have been used to form hydrogels for the controlled delivery of plasmid DNA [92, 106, 107] and adenoviral vectors [92, 108–114], among other model drugs and macromolecules [93, 94]. This approach has been particularly effective for adenoviral gene therapy for cancer treatment as silk-elastin-like protein polymer hydrogels loaded with adenovirus demonstrated greater reduction in tumor volume as compared to control injections of adenovirus in saline solution in a mouse model [113, 114]. In addition to their efficacy, silk-elastin-like protein polymers offer several advantages over other synthetic and natural polymer delivery systems including control of monomer structure at the genetic level and aqueous compatibility for adenoviral viability [114]. In addition, from a processing and delivery perspective, these polymers may be engineered to form thermosensitive hydrogels (liquid at room temperature and hydrogel at body temperature), an attractive feature for any injectable system application [94, 108, 115].

Small molecule drug delivery—For small molecular weight drugs, proof of concept approaches to silk-based drug delivery have primarily focused on film coatings and reservoir systems (Table 4). By controlling the number and thickness of coating layers, as well as silk crystallinity and corresponding film solubility and swelling, a barrier to diffusion is established, and subsequent release rates of the drugs are regulated [10]. One basic approach is to dip coat (as in layer-by-layer assembly) small molecule drug pellets (e.g., approximately 1 cm in diameter) with silk fibroin solution followed by controlled drying and film treatment to manipulate the fibroin crystal form. This has been done using theophylline [116] and adenosine [96], with release profiles lasting from a few hours to 10+ days, respectively, depending on the thickness of the silk film coating, cross-linking with polyethylene glycol, and/or film treatment conditions to control crystallinity. Release rates were primarily a function of coating thickness and crystallinity, with zero order release sustained for up to 17 days [96]. Further control may be achieved by incorporating protease inhibitors into the reservoirs to control local degradation rates [117]. Other reservoir-type approaches include silk fibroin-coated liposomes (300–400 nm), where the introduction of silk fibroin enhanced retention time and improved efficacy for the anti-cancer agent emodin [97, 118]. In addition to reservoir coatings, small molecule drugs may be directly incorporated homogeneously into silk nanolayer coatings for controlled drug delivery [98]. By coating with multiple silk capping layers, and by increasing the silk II, β-sheet crystal content, the initial burst of the model compound rhodamine was suppressed and the duration of release was prolonged up to 30 days [98]. This approach was further validated by incorporating antiproliferative and antithrombotic small molecule drugs, paclitaxel and clopidogrel, into layer-by-layer silk coatings for vascular stents [119]. Pharmacodynamic activity of the coatings was confirmed *in vitro* as the proliferation of human coronary artery smooth muscle cells and human aortic endothelial cells was inhibited over 28 days, indicating concomitant sustained release over that time [119]. In each of these studies, manipulation of the barrier to diffusion through silk fibroin film thickness, crystal form, and crystal content was critical to control the release profile. Additional manipulation of the silk fibroin diffusive barrier may be achieved by increasing the alkali-heat degumming time during silk fibroin purification [91]. For example, it was hypothesized that the lower average fibroin molecular weight due to prolonged alkali-heat degumming led to a less organized

and more permeable fibroin film structure, resulting in faster small molecule drug diffusion [91]. An investigation of specific fibroin physicochemical properties that depend on alkali-heat degumming time may further support this argument, potentially allowing for fine tuning of diffusion-based mechanisms of small molecule release.

Similar control mechanisms may be applied to other silk-based technologies (e.g., microspheres, hydrogels, or combination approaches) to tune the release of small molecules. As an example, silk fibroin microsphere formulations of salicylic acid and propranolol hydrochloride demonstrated approximately first order release kinetics and lower initial burst and sustained release rates at higher concentrations of silk fibroin, with overall release lasting from 1 to 30 days [34]. Silk fibroin microspheres may also be incorporated as part of a fibroin scaffold as a combination approach. For example, adenosine-loaded silk fibroin microspheres were homogenously encapsulated within a porous 3D silk scaffold which in turn was coated with alternating nanolayers of silk fibroin and silk-fibroin-drug films to create additional diffusion barriers. The pharmacodynamic effect of these scaffolds was evaluated in a rat model of kindling epileptogenesis, demonstrating a dose dependent retardation of kindling seizures [120]. Future work on fibroin-based combination formulations should concentrate on reducing system complexity and overall size to avoid issues with reproducibility or invasiveness and enhance the viability of any future implant product. More recent work has focused on incorporation of antibiotics into various silk fibroin-based formats, including films, coatings, microspheres, and hydrogels [99]. For antibiotics with high aqueous solubility (penicillin, ampicillin, cefazolin, gentamicin), release durations were relatively short (1 to 5 days) across all formats (films, nanofilm-coated scaffolds, hydrogels, microsphere-loaded gels), yet still preserved antibiotic efficacy as demonstrated through *in vitro* and *in vivo* testing of bacterial growth. For antibiotics with lower aqueous solubility (rifampicin, erythromycin), longer release durations were achieved (9 and 31 days for rifampicin- and erythromycin-loaded silk sponges, respectively), demonstrating the important role of hydrophobic interactions between the silk and drug in controlling release in a non-diffusion-based mechanism [99]. Further utility of silk fibroin-based small molecule drug delivery was demonstrated using other material formats, such as tetracycline or methylene blue-loaded silk microneedles [73, 121]. As with silk fibroin films, small molecule diffusivity in silk hydrogels can be controlled effectively via varying molecular weight and/or use of other excipients, as demonstrated in buprenorphine-loaded silk protein polymer hydrogels [122], presumably via mechanisms including hydrogel mesh size distribution and intermolecular interactions between the drug and silk matrix.

Biological drug delivery—For biological drug delivery from silk fibroin-based vehicles, significant research has focused on the delivery of growth factors for tissue engineering applications or the delivery of model drugs for proof-of-principle drug delivery applications (Table 5). As with small molecules, the intermolecular interactions between the biological drug and silk fibroin matrix are critical for controlling diffusion-based and more complex release mechanisms. In the most basic silk-based biological drug delivery formulations, adsorption may be used to load preformed, unmodified silk scaffolds with a growth factor of interest by soaking them in a growth factor solution. As an example, this method has been used to load silk fibroin films and electrospun mats with epidermal growth factor (EGF) for

wound healing applications [123]. Growth factor adsorption has also been used to form osteoconductive matrices by coating 3D silk scaffolds with bone morphogenic protein-2 (BMP-2) [81, 100] or BMP-7 adenovirus [124]. In these cases, surface adsorption of the compound of interest is needed to enhance the biological interactions at the cell-biomaterial interface. For sustained drug delivery, however, bulk-loading of formulations by directly mixing the growth factor and silk fibroin solutions prior to formation of the delivery vehicle has generally been the preferred approach, with the exception of lysozyme-coated silk particles [125]. Examples of the solution state loading approach include dextran-, lysozyme-, or horseradish peroxidase (HRP)-loaded silk films [126]; BMP-loaded silk microspheres [127] or electrospun scaffolds [128]; EGF-loaded silk films or electrospun mats [123, 129]; neurotrophin-loaded silk films, tubes [130, 131], or hydrogels [132]; or azoalbumin-loaded [98] or heparin-loaded [119] layer-by-layer silk film coatings. This method of pre-mixing silk and drug before formation has similarly been applied to deliver insulin-like growth factor I (IGF-I) from silk microspheres [34] and 3D scaffolds [101]. Despite differences in material format, these formulations demonstrate the critical role of treatment conditions to induce β-sheet formation and control diffusive pathways, with methanol or water vapor exposure reducing initial burst release and extended release out to 49 and 29 days, respectively [34, 101]. Similar control of crystalline content of horseradish peroxidase (HRP)-loaded silk fibroin microspheres through methanol or salt treatment had a significant effect on release kinetics [32]. As with small molecule delivery, precise control of silk fibroin crystallinity using different processing conditions (e.g., methanol, water annealing, or salt treatment) is critical to manipulate diffusion barriers to achieve target sustained release rates from silk-based formats for a given application.

Additional points of control include format dimensions and intermolecular interactions between the silk fibroin and drug compound of interest. As an example, development of silk micro- and nanospheres using a silk/polyvinyl alcohol (PVA)-based emulsion approach yielded particles with improved control over size and shape [33]. The homogeneity of drug distribution within fibroin spheres, loading efficiency, and the release kinetics of model drugs, e.g. tetramethylrhodamine conjugated dextran and bovine serum albumin (BSA), was a function of silk-drug interactions as dictated by hydrophobicity and surface charge, as well as drug molecular weight [33]. The role of intermolecular interactions on pharmacokinetics has also been observed with silk hydrogels and lyophilized silk hydrogels (lyogels) in the sustained delivery of monoclonal antibodies [102]. While hydrogel preparations released the antibody load relatively rapidly (over 10 days), lyogels with greater than 6.2% (w/w) initial silk fibroin content demonstrated sustained release over 38 days [102]. This release profile was primarily attributed to hydrophobic interactions between the silk fibroin matrix and the antibody as well as the density and crystalline content of the fibroin matrix [41, 102]. Generally, interactions between a target protein drug and the silk fibroin matrix, including size exclusion effects (hydrodynamic radius of the drug vs. effective correlation lengths in the silk matrix), solution state structure of the protein drug, and hydrophobic and electrostatic interactions depending on protein sequence and surface charge, may affect release mechanisms. Thus it is critical to manipulate the properties of the silk matrix to control intermolecular interactions and achieve the desired release profile as a function of a complex combination of diffusion, desorption, and degradation-based release mechanisms.

Silk fibroin structure can be chemically modified to enhance silk-drug intermolecular interactions using various techniques. For example, BMP-2 immobilized on the surface of carbodiimide-coupled silk fibroin films retained biological function as indicated by the differentiation of bone marrow stromal cells [133]. A similar approach was also used to couple NeutrAvidin to silk fibroin in solution or to silk fibroin microspheres as a tool for secondary coupling of antibodies for drug delivery or cell targeting [134]. Alternatively, diazonium coupling chemistry was used to form sulfonated silk fibroin films that improved binding of fibroblast growth factor 2 (FGF-2) [44]. As another example, insulin was covalently coupled to silk fibroin in solution [45] or as nanoparticles [135] using gluteraldehyde as a cross-linking reagent. While effective, these approaches have the drawback of using harsh chemicals that may not be suitable for all biological drugs or drug delivery applications.

As with delivery of small molecule drugs, silk fibroin composite formulation approaches have also been employed for biological drug delivery. These include either all-silk composites of different formats such as glial cell line-derived neurotrophic factor (GDNF)-loaded microspheres within a silk conduit for peripheral nerve repair [136] or blends of silk fibroin with other polymers, such as silk-hyaluronan-based composite hydrogels [137] or an injectable calcium phosphate/silk fibroin/BMP-2 cement for spinal fusion [138]. In some cases, the additional polymer was used as a substrate for silk fibroin coatings as HRP and tetramethylrhodamine-conjugated BSA was delivered for 30 and 16 days, respectively, using PLGA and alginate microspheres coated with silk fibroin to control diffusion-based release [139]. Further studies on silk fibroin composite systems included silk fibroin/gelatin multi-layer films for controlled release of FITC-inulin and FITC-bovine serum albumin (FTIC-BSA) [140] and silk fibroin/polyacrylamide hydrogels for delivery of FITC-inulin [141]. In each case, release kinetics was a function of composition and introduction of a degradation-based release mechanism. More specifically, modulation of the respective ratios of silk fibroin/gelatin or silk fibroin/polyacrylamide and their corresponding polymer degradation rates was used to achieve release up to 28 and 45 days, respectively [140, 141]. The polymer composite approach presents further control of silk-based material properties such as biodegradation rate or swelling ratio, though care must be taken to maintain the biocompatibility and bioactivity of the formulation if synthetic polymers are used.

More complex systems were developed by using combinations of biological or synthetic polymers and material formats as part of silk fibroin-based formulations. These include 3D porous silk scaffolds embedded with FITC-inulin- and BSA-loaded calcium alginate or calcium alginate/silk fibroin-blended beads [142] or IGF-1-loaded PLGA microspheres [143]. These systems utilized silk fibroin scaffold matrix as a diffusion barrier, using silk fibroin concentration and crystallinity as the key parameters to limit burst and prolong release from the embedded drug-loaded microspheres. As another example, BMP-2 and IGF-1 were loaded into silk fibroin and PLGA microspheres, which were subsequently loaded into alginate gels or porous silk fibroin scaffolds to form a gradient for osteochondral tissue engineering [103]. Based on the osteogenic differentiation of human mesenchymal stem cells in the alginate gel system, silk fibroin microspheres were more efficient at delivering BMP-2 than PLGA microspheres, perhaps due to faster release from PLGA spheres or loss of bioactivity due to local acidic microenvironment caused by PLGA

degradation [103]. Taken together, silk fibroin offers a versatile toolkit for various drug delivery applications. This includes not only varied material formats from injectable particles and hydrogels to implantable reservoirs and scaffolds, but also formulation control points from genetic modifications and bioconjugates to material composition and crystallinity. By properly matching the physicochemical properties of the target drug with those of the silk format, near-zero order sustained release may be achieved as a function of diffusion- and degradation-based release mechanisms.

3.2. Mechanisms and modeling

There has been a considerable amount of effort applied to determining the mechanisms of drug release from different silk-based formulations. Through a mechanistic understanding of release kinetics, critical control points in the formulation development may be elucidated to offer guidance for generating near zero-order, silk-based sustained release formulations. Based on the extensive number of applications of silk technology for drug delivery outlined above, most concluded that diffusion or a combination of diffusion, polymer swelling, and polymer degradation are the primary mechanisms governing the release of drug from silk-based formats [96, 101, 127, 144].

In order to describe drug mass transport in diffusion-controlled release, mechanistic mathematical models such as Fick's laws of diffusion can be applied:

$$J_A = -D\frac{dC_A}{dx} \quad (1)$$

$$\frac{dC_A}{dt} = D\frac{d^2C_A}{dx^2} \quad (2)$$

Here, J_A is the diffusive flux of the drug, D is the diffusion coefficient, C_A is the concentration of drug in the release medium, and x and t stand for position and time, respectively [145, 146]. In each of these cases, model assumptions such as a constant drug diffusion coefficient, initial drug concentration below drug solubility, and perfect sink conditions, among others, must be satisfied. Variations in this model have been derived for a variety of geometries including thin films (with negligible edge effects), spheres, and cylinders [145–147]. More complex mechanistic models consider polymer swelling, polymer/drug dissolution, chemically-controlled delivery, and/or polymer erosion/degradation [145–147], but these models have yet to be fully implemented for silk-based delivery systems.

While not based on true release mechanisms, empirical or semi-empirical mathematical models such as the Peppas power law model are useful to compare the general effects of different formulation parameters on release kinetics [146–150]. The Peppas equation is defined as:

$$\frac{M_t}{M_\infty} = kt^n \quad (3)$$

where M_t and M_∞ are the cumulative amount of drug released at time t and infinite time, respectively, k is constant specific to the drug delivery system, and n is the release exponent [147]. Upon fitting the initial release profile (≤60% cumulative release) to the Peppas equation, the drug release mechanism may be elucidated based on the value of the exponent, n. In the case of a thin film, if $n = 0.5$, the release mechanism is Fickian diffusion, and, if $n = 1$, zero order release is observed and polymer swelling is the sole release mechanism. For values of n between 0.5 and 1, anomalous transport is attributed as the release mechanism, due to a combination of drug diffusion as well as polymer swelling and degradation [147]. This power law has similarly been applied to different geometries with different values for n corresponding to different drug release mechanisms [147, 149, 150].

Release mechanisms for small molecule drugs—For studying controlled release of small molecules from silk fibroin formulations, most research has focused on the release of compounds from silk fibroin films with varied crystalline structure. In one study, synthetic dyes were incorporated into silk fibroin films under different processing conditions (untreated, water-annealed to induce *silk I* crystallinity, and methanol-treated to induce *silk II* crystallinity) [151]. The library of dyes included different chemical structures with properties spanning a range of water solubility (logS), hydrophobicity (logP), aqueous conductivity, and net ionic charge, the parameters generally viewed to be critical in determining release kinetics from polymeric release systems [151]. In this particular study, silk fibroin films were chosen as the delivery matrix for ease of fabrication, treatment, and modeling. Dyes were tested for binding to as well as release from the silk fibroin films, and among the 12 small molecule dyes studied (with molecular weights ranging from 291 to 826 g/mol), only three dyes (eosin y sodium salt, brilliant blue R, and methyl red sodium salt) bound to silk and only one dye (brilliant blue R), the dye with the greatest molecular weight and logP among those tested, demonstrated a release mechanism other than simple diffusion [151]. In this case, mathematical modeling of the release indicated a more complex desorption and diffusion release mechanism whereas Fickian diffusion was the primary release mechanism for all other dyes. Within this data set, trends such as increasing diffusion coefficients with increasing water solubility or drug loading as well as decreasing logP or net ionic charge indicated the important role of physicochemical factors, in particular hydrophobic interactions, in determining the release rate. Electrostatic interactions also play a role in controlling release kinetics as silk fibroin, owing to its isoelectric point of ≈4, is negatively charged at neutral pH. Thus, negatively charged molecules generally released faster than positively charged molecules apparently due to electrostatic repulsion. Furthermore, controlling silk fibroin physicochemistry, such as the crystal form and content through methanol-treatment or water-annealing, reduced the effective diffusion coefficients [151]. While this study looked at short-term (less than 1 day) release profiles, similar Fickian diffusion was also observed in longer-term studies (up to 30 days) of sustained release of rhodamine from multi-layered silk fibroin coatings [98].

With additional formulation complexity, e.g. through silk-polymer composites or geometries beyond 2D films, other release mechanisms come into play. As an example, work with silk-gelatin films showed that the release of varied molecular weight compounds was essentially diffusion-controlled over the first 2–3 days, while a second, degradation-controlled phase

was observed for the remainder of the 28-day study [140]. Using the Peppas power law equation, the release mechanism was defined as anomalous transport, involving a combination of drug diffusion as well as polymer swelling and degradation [140]. Similarly, application of the Peppas model to silk fibroin-coated adenosine reservoirs indicated a complex release mechanism with an increase in the exponent, *n*, of the Peppas equation with increasing film thickness [96]. Based on these results, silk fibroin film thickness, crystal form, and crystal content can be viewed as some of the key parameters controlling diffusion in silk fibroin reservoir systems.

Release mechanisms for biological drugs—In terms of biological drug delivery, the physicochemical properties of the silk-based matrix and drug compound as well as their intermolecular interactions dictate release kinetics and mechanisms. For biologicals, the molecular weight of the compound is of particular importance. As an example, silk fibroin films loaded with different molecular weight FITC-dextrans (4 to 40 kDa) were used to evaluate release mechanisms as modeled by modified versions of the Peppas equation and the Fickian diffusion model for porous films [144]. Fitting the sustained release data using the Peppas equation, diffusion was the main release mechanism for FITC-dextrans from silk fibroin films, with a decrease in the effective diffusion coefficient values with increasing molecular weight of the FITC-dextrans. This coincided with a decrease in the cumulative percentage of drug released with increasing molecular weight, presumably due to hydrodynamic size of the model drug approaching the effective network correlation length, demonstrating that the molecular weight of a diffusing solute has a major influence on release from silk matrices [144]. In addition to molecular weight, the role of hydrophobic interactions as a release mechanism has been demonstrated in studies of silk hydrogels and lyogels loaded with monoclonal antibodies [41]. For antibody release, drug delivery was primarily controlled by hydrophobic interactions and hydration resistance over *in vitro* release periods of up to 80 days. These variables were controlled by increasing silk concentration and compressing the silk lyogels to increase silk density. With increased silk density, solvent penetration is limited, thus inhibiting the ability to disrupt the hydrophobic silk-antibody interactions that control release [41].

In general, for both small molecules and biological drugs, physicochemical properties of silk-based formulations (e.g., crystallinity, concentration, density, etc.) are modified to primarily control diffusion-based release mechanisms with some consideration for the long-term effects on biodegradation profiles. According to the Fickian diffusion model, zero order release may be achieved using a silk-based reservoir system. For bulk-loaded systems, however, the time dependence of strictly diffusion-controlled release mandates that true zero order release cannot be realized. Thus, other release mechanisms such as matrix degradation must be combined with diffusion in order to achieve zero order release [144]. This is not unique to silk formulations, as the release profile for PLGA-based products is a complex multiphase process involving solvent penetration, diffusion controlled release, and degradation of the polymer matrix [144]. However, unlike PLGA where the hydrolytic degradation of the matrix is homogeneous in the macroscopic scale (bulk biodegradation), silk-based materials predominantly display heterogeneous, surface-mediated enzymatic biodegradation due to their predominantly hydrophobic nature. In addition to the potential

benefits of heterogeneous biodegradation of silk-based materials in terms of drug stability as discussed in subsection 2.5, the silk biodegradation mechanism is also favorable in terms of pharmacokinetics. For example, strong intermolecular interactions between a drug molecule and the silk-based matrix can be engineered through control of silk physicochemical properties leading to essentially permanent, physical drug binding to the silk-based matrix. Subsequent enzymatic surface biodegradation of the silk-based matrix may result in essentially zero order release of strongly bound drug molecules, in a similar fashion to that observed for pendant chain systems [146]. For silk preparations, controlling degradation-based release kinetics revolves around controlling material format and treatment conditions. For example, using an *in vivo* rat model, aqueous-derived silk scaffolds degraded to completion between 2 to 6 months as opposed to those prepared using hexafluoroisopropanol (HFIP) lasting beyond 1 year [15]. This degradation-controlled sustained drug release mechanism has been demonstrated in an *in vitro* model of basic fibroblast growth factor (bFGF) delivery from aqueous- and HFIP-derived silk scaffolds. In this study, release rates significantly increased with the addition of a proteolytic enzyme to the release medium, with the aqueous-based scaffolds demonstrating a higher increase in release rate due to a higher rate of degradation compared to the organic-derived scaffold [152]. Upon implantation *in vivo*, however, even though the silk scaffolds showed significant improvement in release duration compared to solution control, there was little difference in the degradation or bFGF release profile between the aqueous- and HFIP-derived silk scaffolds, likely due to the short study duration (26 days) not allowing for adequate degradation [152].

Additional control points for silk degradation include alterations to the silk preparation conditions such as increased degumming time, which results in a decrease in molecular weight and an increase in diffusivity and degradation rate [91]. The degradation rates may also be controlled by blending additional polymers in silk hydrogels [141] or layering in silk films [140]. For gelatin-silk films in particular, degradation increased with gelatin content and subsequent release data fit to the Peppas equation demonstrated a corresponding increase in the exponent, *n*, value, indicating more degradation-based release [140]. Overall, future silk-based sustained delivery research should target engineering formulations that combine both the diffusion- and degradation-based mechanisms to achieve zero order release. Because silk enzymatic degradation is desirably a heterogeneous, surface-mediated process, biodegradation rates may be estimated based on silk material format and physicochemical characteristics, enhancing overall predictability of sustained release profiles [139].

3.3. Drug stabilization with silk

As evidenced by a number of sustained release silk-based formulations outlined above, silk plays a role in stabilizing small molecule or biological therapeutics as a function of adsorption, covalent attachment, entrapment, and/or encapsulation [153] (Table 6). This is a critical component for any sustained release application, as the therapeutic drug must maintain bioactivity throughout the duration of release. In general, with the exception of growth factors loaded onto silk fibroin scaffolds by adsorption or covalent coupling of proteins to silk fibroin molecules as described in previous sections, the majority of

stabilization approaches have involved homogeneous encapsulation of a compound of interest in a silk fibroin matrix. As a straightforward small molecule application, the amphiphilic nature of silk fibroin protein and the resulting high solubility of its hydrophobic domains in aqueous solution were used to stabilize hydrophobic particles or encapsulate poorly water soluble substances such as β-carotene [154]. Other applications include the stabilization of antibiotics such as erythromycin, which is highly unstable in aqueous media, to maintain bioactivity at 37°C for up to 31 days when loaded into a hydrated silk scaffold [99]. This work has been further expanded to include tetracycline- and penicillin-loaded silk fibroin films. Tetracycline-loaded films demonstrated no loss of activity over a 4 week time period when stored at 4°C, 25°C (with or without light exposure), and 37°C, and only a 20% loss of activity when stored at 60°C, a significant improvement in stability over tetracycline solution [31]. Long-term stability of tetracycline in silk fibroin films also compared favorably to the stability of tetracycline in dry powder form for those stored at temperatures between 4–60°C for 6 months or longer [31].

For biological compounds, bulk-drug loaded silk fibroin films, hydrogels, and scaffolds are commonly used for protein and peptide stabilization. Enzyme stabilization is one prominent example of silk stabilization, as improved stability of HRP, glucose oxidase (GOx), and others have been reported [153]. In a series of studies, silk fibroin was able to stabilize and enhance the activity of HRP, a commonly used indicator enzyme that is not stable in aqueous solution. HRP stabilization was achieved with both silk fibroin solution and film formats, with an activity that increased by 30 to 40% and a half-life that extended from 2.5 hours to 25 days at room temperature [30]. For HRP-loaded silk fibroin films, HRP activity immediately after film preparation was approximately 1.2- to 2.4-fold greater than the original activity in solution for non-methanol treated films depending on loading, with methanol-treated films retaining approximately 32% of activity [30, 155]. Similar results were also observed for GOx- and lipase-loaded silk fibroin films [155]. Studies on GOx-loaded silk fibroin films demonstrated greater than 80% activity as compared to the free enzyme for low loading (0.002%) conditions [156] as well as improvements in enzyme thermal and pH stability [156–158]. For long-term storage, enzyme-loaded silk films, including HRP-, lipase-, organophosphorus hydrolase (OPH)-, and GOx-loaded films, have demonstrated significant retention of activity over 5 months to 2 years depending on the specific drug and storage conditions (4°C, room temperature, or 37°C) [155, 159, 160]. In most cases, activity was treatment and formulation dependent, with methanol treatment and lower loading values generally reducing enzyme stability [155]. Based on these results, the mechanism of stabilization in silk is suspected to be due to specific interactions between the enzymes and hydrophobic regions of the silk fibroin, as well as reduced enzyme chain mobility. These enzyme-silk fibroin intermolecular interactions depended on the relative fractions of silk fibroin molecular conformations (e.g., *silk I* and *silk II*) in an enzyme-specific manner. For example, it was proposed that stabilization of hydrophilic or hydrophobic drugs may be better achieved by formats with higher *silk I* or *silk II* crystal content, respectively [161]. In addition, as enzyme activity is not only preserved but also enhanced in silk fibroin solution and films, enzyme interactions with silk fibroin may effectively reverse enzyme denaturation in the aqueous solution [155].

Beyond enzyme-loaded films, silk fibroin formats have also been used to stabilize vaccines and monoclonal antibodies [31, 41, 102]. For vaccine stabilization, silk fibroin films loaded with the measles, mumps, and rubella (MMR) vaccine demonstrated enhanced stability for up to 6 months as compared to that of powder stored at 25°C, 37°C, and 45°C [31]. Vaccine stability was further enhanced by lyophilizing the silk fibroin films, as ≥85% of the initial potency was retained for all vaccine components after six months of storage at both 37°C and 45°C, and the viral half-life of the measles component at 37°C was improved from 9.4 weeks for dry powder to 22.0 weeks or 93.8 weeks for untreated or lyophilized silk films, respectively [31]. This improvement in vaccine thermal stability is attributed to the low residual moisture content within silk fibroin films as well as reduced vaccine chain mobility, raising the effective glass transition temperature of the viral proteins and minimizing temperature-induced protein denaturation and aggregation [31]. For monoclonal antibody-loaded silk fibroin lyogels, no significant change in antibody physical stability, charge heterogeneity or biological function was observed over the sustained release duration [41]. This is in contrast to encapsulation of therapeutic proteins in PLGA nano- or microparticles, where loss of efficacy due to protein degradation or denaturation has been observed due to exposure of the protein drugs to organic solvents during particle processing or the acidic micro-environment generated due to degradation of the PLGA matrix into acidic byproducts [162]. Prior work with BSA-loaded cylindrical implants and microenvironment simulations also demonstrated that the acidic microclimate created by degradation of PLGA polymer induced denaturation and aggregation of encapsulated BSA, resulting in 50% aggregation within 12 days [163].

4. A proposed early development pathway towards silk-based products

As outlined in this review and others [7–10], a considerable amount of work has been dedicated to the processing and characterization of silk-based drug delivery vehicles. This enthusiasm stems from the unique combination of beneficial properties of silk for drug delivery applications along with validation of the silk technology by FDA-approved silk devices including silk sutures (Surusil®, Suru; Sofsilk™, Covidien) and silk scaffolds (Seri® Surgical Scaffold, Allergan). In terms of silk-based drug delivery, however, the critical path to bringing Good Manufacturing Practice (GMP)-compliant fibroin-based products to the market, while ensuring proper safety, identity, strength, purity and quality remains to be addressed.

In early stage research and bench-scale production, it is essential to develop robust and scalable silk purification and processing steps, as well as to develop analytical tools to enable thorough characterization of silk-based formulations. For example, the exact fibroin purification protocol may have profound effects on the molecular weight distribution, amino acid sequence, self-assembly kinetics, and the crystal polymorphism, resulting in differences in the physicochemical properties and the biological and pharmacological outcomes. Therefore, proper purification process controls should be established to determine the critical silk processing parameters to optimize product identity and purity and achieve desirable pharmaceutical outcomes while ensuring a robust process. The possible means to characterize fibroin product identity and purity on a batch-to-batch basis include morphological analysis of fibroin fiber surfaces, monitoring the degumming yield, amino

acid analysis, and electrophoretic, [17, 24], spectroscopic [164], chromatographic [165, 166], and biological analyses. All testing should be conducted according to Pharmacopeia standards when such standards are available.

With a fully characterized silk as a starting point, a systematic approach should be taken to formulation development, including the selection of a viable drug candidate, appropriate silk material format, and manipulation of the critical processing parameters in order to control pharmacokinetics. In selecting a drug candidate, several factors must be taken into account, including the current market for the specific drug as well as the disease targets. Furthermore, any potential silk-based formulation must be able to demonstrate a significant improvement over existing marketed therapies in clinical outcomes and/or patient compliance in order to be justifiable to third-party payers. There may also be opportunities for silk-based formulations where other polymer approaches have failed due to their inherent limitations (e.g., protein stability issues or requirement of organic solvents for PLGA).

Upon identifying a clinical need, the drug of interest must have sufficient potency to enable development of a sustained release product, considering practical limitations on dose (e.g. ≤ 5 mm in diameter for an implant, ≤ 2 ml or ≤ 5 ml for a subcutaneous or an intramuscular injection, respectively) and drug-specific loading efficiency. Products with high therapeutic thresholds (and large daily doses), for example, would require impractically large implant depots. Beyond potency, possible influence of drug physicochemical properties, e.g., hydrophobicity, charge state and density, molecular weight, and resulting strength or lifetime of silk-drug interactions on pharmacokinetics should be considered. While silk-drug interactions could be tuned through silk sequence modifications, silk is negatively charged at neutral pH and thus compounds with higher isoelectric points have generally demonstrated enhanced sustained release [167]. Similarly, due to the hydrophobic nature of silk, compounds with moderate to high hydrophobicity and low aqueous solubility have generally performed better [151].

For formulation development, different approaches should be taken for small molecule or biological therapeutics. For small molecules, the majority of research has focused on dense, crystalline silk films or coatings with high hydration resistance and relatively low swelling ratios to obtain silk network correlation lengths comparable to that of the drug molecule. For macromolecules, on the other hand, a variety of injectable, hydrated formulations with high effective specific surface area (e.g., hydrogels, micro- and nanosphere suspensions) have been investigated. Furthermore, the exact mechanism of release for each drug candidate must be taken into consideration during sustained release product development. For silk-based, small molecule drug formulations, the release mechanism may be largely diffusion-based, with inverse relationships between the release rate and formulation parameters such as the silk matrix thickness, silk-to-drug mass ratio, characteristic size of the matrix, and the strength of silk-drug interactions. Though generally not the release-controlling mechanism in small molecule delivery, the possible influence of silk biodegradation rates on the release kinetics should also be considered. For protein-loaded silk products, the release mechanism can be single or multi-modal including distinct regimes for silk matrix swelling, drug diffusion and silk matrix biodegradation. Following diffusive release kinetics controlled by size exclusion effects, and the finite lifetime of specific silk-macromolecule interactions,

macromolecules that are essentially permanently bound to the silk matrix could be released as a function of silk biodegradation [161]. Additionally, with any silk-based formulation, immediate (burst) release may result from incomplete drug encapsulation and phase separation events during formulation processing. The formulation development must consider all of these aspects to optimize encapsulation and diffusion-controlled release, while considering the controllable biodegradation of silk materials. As with any drug product development, it is also critical to conduct comprehensive *in vivo* pharmacokinetic assays on silk-based formats until an *in vitro-in vivo* correlation is established, especially considering that silk-based formulations will be subject to surface-mediated, enzymatic biodegradation unlike hydrolytically degrading PLGA polymers in bulk. Overall, an iterative and systematic approach should enable near-zero order release kinetics from silk-based formulations through careful control of various release mechanisms.

Acknowledgments

This work was supported by a sponsored research agreement between Tufts University and Ekteino Laboratories, Inc. We thank Dr. Danielle Rockwood for kindly providing the silk scaffold SEM image in figure 3.

References

1. Mao S, Guo C, Shi Y, Li LC. Recent advances in polymeric microspheres for parenteral drug delivery part 1, Expert Opinion on Drug Delivery. 2012; 9:1161–1176.
2. Estey T, Kang J, Schwendeman SP, Carpenter JF. BSA degradation under acidic conditions: A model for protein instability during release from PLGA delivery systems. Journal of Pharmaceutical Sciences. 2006; 95:1626–1639. [PubMed: 16729268]
3. Giteau A, Venier-Julienne MC, Aubert-Pouessel A, Benoit JP. How to achieve sustained and complete protein release from PLGA-based microparticles? International Journal of Pharmaceutics. 2008; 350:14–26. [PubMed: 18162341]
4. Tamber H, Johansen P, Merkle HP, Gander B. Formulation aspects of biodegradable polymeric microspheres for antigen delivery. Advanced Drug Delivery Reviews. 2005; 57:357–376. [PubMed: 15560946]
5. Van Der Walle CF, Sharma G, Kumar MNVR. Current approaches to stabilising and analysing proteins during microencapsulation in PLGA. Expert Opinion on Drug Delivery. 2009; 6:177–186. [PubMed: 19239389]
6. Elzoghby AO, Samy WM, Elgindy NA. Protein-based nanocarriers as promising drug and gene delivery systems. Journal of Controlled Release. 2012; 161:38–49. [PubMed: 22564368]
7. Meinel L, Kaplan DL. Silk constructs for delivery of musculoskeletal therapeutics. Advanced Drug Delivery Reviews. 2012; 64:1111–1122. [PubMed: 22522139]
8. Numata K, Kaplan DL. Silk-based delivery systems of bioactive molecules. Adv Drug Deliv Rev. 2010; 62:1497–1508. [PubMed: 20298729]
9. Pritchard EM, Kaplan DL. Silk fibroin biomaterials for controlled release drug delivery. Expert Opinion on Drug Delivery. 2011; 8:797–811. [PubMed: 21453189]
10. Wenk E, Merkle HP, Meinel L. Silk fibroin as a vehicle for drug delivery applications. Journal of Controlled Release. 2011; 150:128–141. [PubMed: 21059377]
11. Diab T, Pritchard EM, Uhrig BA, Boerckel JD, Kaplan DL, Guldberg RE. A silk hydrogel-based delivery system of bone morphogenetic protein for the treatment of large bone defects. Journal of the Mechanical Behavior of Biomedical Materials. 2012; 11:123–131. [PubMed: 22658161]
12. Horan RL, Toponarski I, Boepple HE, Weitzel PP, Richmond JC, Altman GH. Design and characterization of a scaffold for anterior cruciate ligament engineering. The journal of knee surgery. 2009; 22:82–92. [PubMed: 19216356]

13. Numata K, Cebe P, Kaplan DL. Mechanism of enzymatic degradation of beta-sheet crystals. Biomaterials. 2010; 31:2926–2933. [PubMed: 20044136]
14. Rajkhowa R, Hu X, Tsuzuki T, Kaplan DL, Wang X. Structure and biodegradation mechanism of milled Bombyx mori silk particles. Biomacromolecules. 2012; 13:2503–2512. [PubMed: 22746375]
15. Wang Y, Rudym DD, Walsh A, Abrahamsen L, Kim HJ, Kim HS, Kirker-Head C, Kaplan DL. In vivo degradation of three-dimensional silk fibroin scaffolds. Biomaterials. 2008; 29:3415–3428. [PubMed: 18502501]
16. Altman GH, Diaz F, Jakuba C, Calabro T, Horan RL, Chen JS, Lu H, Richmond J, Kaplan DL. Silk-based Biomaterials. Biomaterials. 2003; 24:401–416. [PubMed: 12423595]
17. Altman, GH.; Horan, RL.; Collette, AL.; Chen, J. Silk Fibroin Hydrogels and Uses Thereof. US 2011/0020409. 2011.
18. Fini M, Motta A, Torricelli P, Glavaresi G, Aldini NN, Tschon M, Giardino R, Migliaresi C. The healing of confined critical size cancellous defects in the presence of silk fibroin hydrogel. Biomaterials. 2005; 26:3527–3536. [PubMed: 15621243]
19. Horan RL, Bramono DS, Stanley JRL, Simmons Q, Chen J, Boepple HE, Altman GH. Biological and biomechanical assessment of a long-term bioresorbable silk-derived surgical mesh in an abdominal body wall defect model. Hernia. 2009; 13:189–199. [PubMed: 19198755]
20. Meinel L, Hofmann S, Karageorgiou V, Kirker-Head C, McCool J, Gronowicz G, Zichner L, Langer R, Vunjak-Novakovic G, Kaplan DL. The inflammatory responses to silk films in vitro and in vivo. Biomaterials. 2005; 26:147–155. [PubMed: 15207461]
21. Panilaitis B, Altman GH, Chen J, Jin HJ, Karageorgiou V, Kaplan DL. Macrophage responses to silk. Biomaterials. 2003; 24:3079–3085. [PubMed: 12895580]
22. Santin M, Motta A, Freddi G, Cannas M. In vitro evaluation of the inflammatory potential of the silk fibroin. J Biomed Mater Res. 1999; 46:382–389. [PubMed: 10397996]
23. Seib FP, Maitz MF, Hu X, Werner C, Kaplan DL. Impact of processing parameters on the haemocompatibility of Bombyx mori silk films. Biomaterials. 2012; 33:1017–1023. [PubMed: 22079005]
24. Wray LS, Hu X, Gallego J, Georgakoudi I, Omenetto FG, Schmidt D, Kaplan DL. Effect of processing on silk-based biomaterials: reproducibility and biocompatibility. J Biomed Mater Res B Appl Biomater. 2011; 99:89–101. [PubMed: 21695778]
25. Rockwood DN, Preda RC, Yucel T, Wang X, Lovett ML, Kaplan DL. Materials fabrication from Bombyx mori silk fibroin. Nature Protocols. 2011; 6:1612–1631.
26. George KA, Shadforth AMA, Chirila TV, Laurent MJ, Stephenson SA, Edwards GA, Madden PW, Hutmacher DW, Harkin DG. Effect of the sterilization method on the properties of Bombyx mori silk fibroin films. Materials Science and Engineering C. 2013; 33:668–674.
27. Gil ES, Park SH, Hu X, Cebe P, Kaplan DL. Impact of Sterilization on the Enzymatic Degradation and Mechanical Properties of Silk Biomaterials. Macromolecular Bioscience. 2013
28. Hedhammar M, Bramfeldt H, Baris T, Widhe M, Askarieh G, Nordling K, Aulock S, Johansson J. Sterilized recombinant spider silk fibers of low pyrogenicity. Biomacromolecules. 2010; 11:953–959. [PubMed: 20235574]
29. Wu X, Mao L, Qin D, Lu S. Impact of sterilization methods on the stability of silk fibroin solution. Guangzhou. 2011:1755–1759.
30. Lu SZ, Wang XQ, Uppal N, Kaplan DL, Li MZ. Stabilization of horseradish peroxidase in silk materials. Frontiers of Materials Science in China. 2009; 3:367–373.
31. Zhang J, Pritchard E, Hu X, Valentin T, Panilaitis B, Omenetto FG, Kaplan DL. Stabilization of vaccines and antibiotics in silk and eliminating the cold chain. Proceedings of the National Academy of Sciences of the United States of America. 2012; 109:11981–11986. [PubMed: 22778443]
32. Wang XQ, Wenk E, Matsumoto A, Meinel L, Li CM, Kaplan DL. Silk microspheres for encapsulation and controlled release. Journal of Controlled Release. 2007; 117:360–370. [PubMed: 17218036]
33. Wang XQ, Yucel T, Lu Q, Hu X, Kaplan DL. Silk Nanospheres and Microspheres from Silk/PVA Blend Films for Drug Delivery. Biomaterials. 2010; 31:1025–1035. [PubMed: 19945157]

34. Wenk E, Wandrey AJ, Merkle HP, Meinel L. Silk fibroin spheres as a platform for controlled drug delivery. J Control Release. 2008; 132:26–34. [PubMed: 18761384]
35. Leisk GG, Lo TJ, Yucel T, Lu Q, Kaplan DL. Electrogelation for Protein Adhesives. Advanced Materials. 2010; 22:711–715. [PubMed: 20217775]
36. Yucel T, Kojic N, Leisk GG, Lo TJ, Kaplan DL. Non-equilibrium Silk Fibroin Adhesives. Journal of Structural Biology. 2010; 170:406–412. [PubMed: 20026216]
37. Kim UJ, Park JY, Li CM, Jin HJ, Valluzzi R, Kaplan DL. Structure and properties of silk hydrogels. Biomacromolecules. 2004; 5:786–792. [PubMed: 15132662]
38. Wang XQ, Kluge JA, Leisk GG, Kaplan DL. Sonication-induced Gelation of Silk Fibroin for Cell Encapsulation. Biomaterials. 2008; 29:1054–1064. [PubMed: 18031805]
39. Yucel T, Cebe P, Kaplan DL. Vortex-induced injectable silk fibroin hydrogels. Biophysical Journal. 2009; 97:2044–2050. [PubMed: 19804736]
40. Kaplan, DL.; Yucel, T.; Lovett, ML.; Wang, X. Silk Reservoirs for Drug Delivery. WO2013US30206 20130311. 2013.
41. Guziewicz NA, Massetti AJ, Perez-Ramirez BJ, Kaplan DL. Mechanisms of monoclonal antibody stabilization and release from silk biomaterials. Biomaterials. 2013; 34:7766–7775. [PubMed: 23859659]
42. Murphy AR, Kaplan DL. Biomedical applications of chemically-modified silk fibroin. Journal of Materials Chemistry. 2009; 19:6443–6450. [PubMed: 20161439]
43. Numata K, Subramanian B, Currie HA, Kaplan DL. Bioengineered silk protein-based gene delivery systems. Biomaterials. 2009; 30:5775–5784. [PubMed: 19577803]
44. Wenk E, Murphy AR, Kaplan DL, Meinel L, Merkle HP, Uebersax L. The use of sulfonated silk fibroin derivatives to control binding, delivery and potency of FGF-2 in tissue regeneration. Biomaterials. 2010; 31:1403–1413. [PubMed: 19942287]
45. Zhang YQ, Ma Y, Xia YY, Shen WD, Mao JP, Zha XM, Shirai K, Kiguchi K. Synthesis of silk fibroin-insulin bioconjugates and their characterization and activities in vivo. Journal of Biomedical Materials Research - Part B Applied Biomaterials. 2006; 79:275–283.
46. Hu X, Kaplan D, Cebe P. Dynamic Protein-Water Relationships during β-sheet Formation. Macromolecules. 2008; 41:3939–3948.
47. Jin HJ, Park J, Karageorgiou V, Kim UJ, Valluzzi R, Cebe P, Kaplan DL. Water-stable silk films with reduced β-sheet content. Advanced Functional Materials. 2005; 15:1241–1247.
48. Wilson D, Valluzzi R, Kaplan D. Conformational transitions model silk peptides. Biophysical Journal. 2000; 78:2690–2701. [PubMed: 10777765]
49. Cramer E. Ueber die Bestandtheile der Seide. Journal fur Praktische Chemie. 1865; 65:76–98.
50. Inoue S, Tanaka K, Arisaka F, Kimura S, Ohtomo K, Mizuno S. Silk fibroin of Bombyx mori is secreted assembling a high molecular mass elementary unit consisting of H-chain, L-chain, and P25, with a 6:6:1 molar ratio. Journal of Biological Chemistry. 2000; 275:40517–40528. [PubMed: 10986287]
51. Jin HJ, Kaplan DL. Mechanism of Silk Processing in Insects and Spiders. Nature. 2003; 424:1057–1061. [PubMed: 12944968]
52. Lucas F, Shaw JTB, Smith SG. The Silk Fibroins. Advances in Protein Chemistry. 1958:107–242. [PubMed: 14418664]
53. Marsh RE, Corey RB, Pauling L. An Investigation of the Structure of Silk Fibroin. Biochimica Et Biophysica Acta. 1955; 16:1–34. [PubMed: 14363226]
54. Pauling L, Corey RB. Stable configurations of polypeptide chains. Proceedings of the Royal Society of London. Series B, Containing papers of a Biological character. Royal Society (Great Britain). 1953; 141:21–33.
55. Tanaka K, Kajiyama N, Ishikura K, Waga S, Kikuchi A, Ohtomo K, Takagi T, Mizuno S. Determination of the site of disulfide linkage between heavy and light chains of silk fibroin produced by Bombyx mori. Biochimica et Biophysica Acta - Protein Structure and Molecular Enzymology. 1999; 1432:92–103.

56. Yamaguchi K, Kikuchi Y, Takagi T, Kikuchi A, Oyama F, Shimura K, Mizuno S. Primary structure of the silk fibroin light chain determined by cDNA sequencing and peptide analysis. Journal of Molecular Biology. 1989; 210:127–139. [PubMed: 2585514]
57. Zhou CZ, Confalonieri F, Medina N, Zivanovic Y, Esnault C, Yang T, Jacquet M, Janin J, Duguet M, Perasso R, Li ZG. Fine organization of Bombyx mori fibroin heavy chain gene. Nucleic Acids Research. 2000; 28:2413–2419. [PubMed: 10871375]
58. Zhou C-Z, Confalonieri F, Jacquet M, Perasso R, Li ZG, Janin J. Silk fibroin: Structural implications of a remarkable amino acid sequence. Proteins: Structure, Function, and Bioinformatics. 2001; 44:119–122.
59. Inoue S, Tanaka K, Arisaka F, Kimura S, Ohtomo K, Mizuno S. Silk Fibroin of Bombyx Mori is Secreted, Assembling a High Molecular Mass Elementary Unit Consisting of H-chain, L-chain, and P25, with a 6:6:1 Molar Ratio. Journal of Biological Chemistry. 2000; 275:40517–40528. [PubMed: 10986287]
60. UniProtKB. Universal Protein Resource Accession numbers (Fib-H: P05790; Fib-L: P21828; p25: P04148).
61. Leisk GG, Lo TJ, Yucel T, Lu Q, Kaplan DL. Electrogelation for protein adhesives. Advanced Materials. 22:711–715. [PubMed: 20217775]
62. Asakura T, Suzuki Y, Nakazawa Y, Holland GP, Yarger JL. Elucidating silk structure using solid-state NMR. Soft Matter. 2013; 9:11440–11450.
63. Wilson D, Valluzzi R, Kaplan D. Conformational transitions in model silk peptides. Biophysical Journal. 2000; 78:2690–2701. [PubMed: 10777765]
64. Valluzzi R, Gido SP, Muller W, Kaplan DL. Orientation of silk III at the air-water interface. International Journal of Biological Macromolecules. 1999; 24:237–242. [PubMed: 10342770]
65. Dewair M, Baur X, Ziegler K. Use of immunoblot technique for detection of human IgE and IgG antibodies to individual silk proteins. Journal of Allergy and Clinical Immunology. 1985; 76:537–542. [PubMed: 4056241]
66. Zaoming W, Codina R, Fernandez-Caldas E, Lockey RF. Partial characterization of the silk allergens in mulberry silk extract. Journal of Investigational Allergology and Clinical Immunology. 1996; 6:237–241. [PubMed: 8844500]
67. Takasu Y, Yamada H, Tsubouchi K. Isolation of three main sericin components from the cocoon of the silkworm, Bombyx mori, Bioscience. Biotechnology and Biochemistry. 2002; 66:2715–2718.
68. Gamo T, Inokuchi T, Laufer H. Polypeptides of fibroin and sericin secreted from the different sections of the silk gland in Bombyx mori. Insect Biochemistry. 1977; 7:285–295.
69. Sprague KU. The Bombyx mon silk proteins: Characterization of large polypeptides. Biochemistry. 1975; 14:925–931. [PubMed: 1125178]
70. Dyakonov T, Yang CH, Bush D, Gosangari S, Majuru S, Fatmi A. Design and Characterization of a Silk-Fibroin-Based Drug Delivery Platform Using Naproxen as a Model Drug. Journal of Drug Delivery. 2012; 2012
71. Wang X, Yucel T, Lu Q, Hu X, Kaplan DL. Silk nanospheres and microspheres from silk/pva blend films for drug delivery. Biomaterials. 31:1025–1035. [PubMed: 19945157]
72. Lovett ML, Cannizzaro CM, Vunjak-Novakovic G, Kaplan DL. Gel spinning of silk tubes for tissue engineering. Biomaterials. 2008; 29:4650–4657. [PubMed: 18801570]
73. Tsioris K, Raja WK, Pritchard EM, Panilaitis B, Kaplan DL, Omenetto FG. Fabrication of silk microneedles for controlled-release drug delivery. Advanced Functional Materials. 2011; 22:330–335.
74. Athanasiou KA, Niederauer GG, Agrawal CM. Sterilization, toxicity, biocompatibility and clinical applications of polylactic acid/polyglycolic acid copolymers. Biomaterials. 1996; 17:93–102. [PubMed: 8624401]
75. Wiegand C, Abel M, Ruth P, Wilhelms T, Schulze D, Norgauer J, Hipler UC. Effect of the sterilization method on the performance of collagen type I on chronic wound parameters in vitro. Journal of Biomedical Materials Research - Part B Applied Biomaterials. 2009; 90:710–719.
76. Holy CE, Cheng C, Davies JE, Shoichet MS. Optimizing the sterilization of PLGA scaffolds for use in tissue engineering. Biomaterials. 2001; 22:25–31. [PubMed: 11085380]

77. Hofmann S, Stok KS, Kohler T, Meinel AJ, Müller R. Effect of sterilization on structural and material properties of 3-D silk fibroin scaffolds. Acta Biomaterialia. 2014; 10:308–317. [PubMed: 24013025]

78. Jin HJ, Chen J, Karageorgiou V, Altman GH, Kaplan DL. Human bone marrow stromal cell responses on electrospun silk fibroin mats. Biomaterials. 2004; 25:1039–1047. [PubMed: 14615169]

79. Meinel L, Hofmann S, Betz O, Fajardo R, Merkle HP, Langer R, Evans CH, Vunjak-Novakovic G, Kaplan DL. Osteogenesis by human mesenchymal stem cells cultured on silk biomaterials: Comparison of adenovirus mediated gene transfer and protein delivery of BMP-2. Biomaterials. 2006; 27:4993–5002. [PubMed: 16765437]

80. Motta A, Migliaresi C, Faccioni F, Torricelli P, Fini M, Giardino R. Fibroin hydrogels for biomedical applications: Preparation, characterization and in vitro cell culture studies. Journal of Biomaterials Science. Polymer Edition. 2004; 15:851–864.

81. Kirker-Head C, Karageorgiou V, Hofmann S, Fajardo R, Betz O, Merkle HP, Hilbe M, von Rechenberg B, McCool J, Abrahamsen L, Nazarian A, Cory E, Curtis M, Kaplan D, Meinel L. BMP-silk composite matrices heal critically sized femoral defects. Bone. 2007; 41:247–255. [PubMed: 17553763]

82. Meinel L, Fajardo R, Hofmann S, Langer R, Chen J, Snyder B, Vunjak-Novakovic G, Kaplan D. Silk implants for the healing of critical size bone defects. Bone. 2005; 37:688–698. [PubMed: 16140599]

83. Aramwit P, Kanokpanont S, De-Eknamkul W, Srichana T. Monitoring of inflammatory mediators induced by silk sericin. Journal of Bioscience and Bioengineering. 2009; 107:556–561. [PubMed: 19393558]

84. Aramwit P, Kanokpanont S, Nakpheng T, Srichana T. The effect of sericin from various extraction methods on cell viability and collagen production. International Journal of Molecular Sciences. 2010; 11:2200–2211. [PubMed: 20559510]

85. Kino T, Oshima S. Allergy to insects in Japan. I. The reaginic sensitivity to moth and butterfly in patients with bronchial asthma. Journal of Allergy and Clinical Immunology. 1978; 61:10–16. [PubMed: 618942]

86. Johansson SGO, Wuthrich B, Zortea-Caflisch C. Nightly asthma caused by allergens in silk-filled bed quilts: Clinical and immunologic studies. Journal of Allergy and Clinical Immunology. 1985; 75:452–459. [PubMed: 3980881]

87. Bhattacharjee M, Schultz-Thater E, Trella E, Miot S, Das S, Loparic M, Ray AR, Martin I, Spagnoli GC, Ghosh S. The role of 3D structure and protein conformation on the innate and adaptive immune responses to silk-based biomaterials. Biomaterials. 2013; 34:8161–8171. [PubMed: 23896003]

88. Li M, Ogiso M, Minoura N. Enzymatic degradation behavior of porous silk fibroin sheets. Biomaterials. 2003; 24:357–365. [PubMed: 12419638]

89. Numata K, Kaplan DL. Differences in Cytotoxicity of β-Sheet Peptides Originated from Silk and Amyloid β. Macromolecular Bioscience. 2011; 11:60–64. [PubMed: 20954203]

90. Horan RL, Antle K, Collette AL, Huang YZ, Huang J, Moreau JE, Volloch V, Kaplan DL, Altman GH. In Vitro Degradation of Silk Fibroin. Biomaterials. 2005; 26:3385–3393. [PubMed: 15621227]

91. Pritchard EM, Hu X, Finley V, Kuo CK, Kaplan DL. Effect of Silk Protein Processing on Drug Delivery from Silk Films. Macromolecular Bioscience. 2013; 13:311–320. [PubMed: 23349062]

92. Megeed Z, Haider M, Li D, O'Malley BW Jr, Cappello J, Ghandehari H. In vitro and in vivo evaluation of recombinant silk-elastinlike hydrogels for cancer gene therapy. Journal of Controlled Release. 2004; 94:433–445. [PubMed: 14744493]

93. Megeed Z, Cappello J, Ghandehari H. Genetically engineered silk-elastinlike protein polymers for controlled drug delivery. Advanced Drug Delivery Reviews. 2002; 54:1075–1091. [PubMed: 12384308]

94. Gustafson JA, Ghandehari H. Silk-elastinlike protein polymers for matrix-mediated cancer gene therapy. Advanced Drug Delivery Reviews. 2010; 62:1509–1523. [PubMed: 20430059]

95. Numata K, Reagan MR, Goldstein RH, Rosenblatt M, Kaplan DL. Spider silk-based gene carriers for tumor cell-specific delivery. Bioconjugate Chemistry. 2011; 22:1605–1610. [PubMed: 21739966]

96. Pritchard EM, Szybala C, Boison D, Kaplan DL. Silk fibroin encapsulated powder reservoirs for sustained release of adenosine. Journal of Controlled Release. 2010; 144:159–167. [PubMed: 20138938]

97. Gobin AS, Rhea R, Newman RA, Mathur AB. Silk-fibroin-coated liposomes for long-term and targeted drug delivery. International journal of nanomedicine. 2006; 1:81–87. [PubMed: 17722265]

98. Wang X, Hu X, Daley A, Rabotyagova O, Cebe P, Kaplan DL. Nanolayer biomaterial coatings of silk fibroin for controlled release. J Control Release. 2007; 121:190–199. [PubMed: 17628161]

99. Pritchard EM, Valentin T, Panilaitis B, Omenetto F, Kaplan DL. Antibiotic-releasing silk biomaterials for infection prevention and treatment. Advanced Functional Materials. 2013; 23:854–861. [PubMed: 23483738]

100. Karageorgiou V, Tomkins M, Fajardo R, Meinel L, Snyder B, Wade K, Chen J, Vunjak-Novakovic G, Kaplan DL. Porous silk fibroin 3-D scaffolds for delivery of bone morphogenetic protein-2 in vitro and in vivo. J Biomed Mater Res A. 2006; 78:324–334. [PubMed: 16637042]

101. Uebersax L, Merkle HP, Meinel L. Insulin-like growth factor I releasing silk fibroin scaffolds induce chondrogenic differentiation of human mesenchymal stem cells. J Control Release. 2008; 127:12–21. [PubMed: 18280603]

102. Guziewicz N, Best A, Perez-Ramirez B, Kaplan DL. Lyophilized silk fibroin hydrogels for the sustained local delivery of therapeutic monoclonal antibodies. Biomaterials. 2011; 32:2642–2650. [PubMed: 21216004]

103. Wang X, Wenk E, Zhang X, Meinel L, Vunjak-Novakovic G, Kaplan DL. Growth factor gradients via microsphere delivery in biopolymer scaffolds for osteochondral tissue engineering. J Control Release. 2009; 134:81–90. [PubMed: 19071168]

104. Numata K, Hamasaki J, Subramanian B, Kaplan DL. Gene delivery mediated by recombinant silk proteins containing cationic and cell binding motifs. Journal of Controlled Release. 2010; 146:136–143. [PubMed: 20457191]

105. Numata K, Kaplan DL. Silk-based gene carriers with cell membrane destabilizing peptides. Biomacromolecules. 2010; 11:3189–3195. [PubMed: 20942485]

106. Megeed Z, Cappello J, Ghandehari H. Controlled release of plasmid DNA from a genetically engineered silk-elastinlike hydrogel. Pharmaceutical Research. 2002; 19:954–959. [PubMed: 12180547]

107. Hwang D, Moolchandani V, Dandu R, Haider M, Cappello J, Ghandehari H. Influence of polymer structure and biodegradation on DNA release from silk-elastinlike protein polymer hydrogels. International Journal of Pharmaceutics. 2009; 368:215–219. [PubMed: 19027056]

108. Gustafson J, Greish K, Frandsen J, Cappello J, Ghandehari H. Silk-elastinlike recombinant polymers for gene therapy of head and neck cancer: From molecular definition to controlled gene expression. Journal of Controlled Release. 2009; 140:256–261. [PubMed: 19470397]

109. Gustafson JA, Price RA, Greish K, Cappello J, Ghandehari H. Silk-elastin-like hydrogel improves the safety of adenovirus-mediated gene-directed enzyme-'prodrug therapy. Molecular Pharmaceutics. 2010; 7:1050–1056. [PubMed: 20586469]

110. Hatefi A, Cappello J, Ghandehari H. Adenoviral gene delivery to solid tumors by recombinant silkelastinlike protein polymers. Pharmaceutical Research. 2007; 24:773–779. [PubMed: 17308969]

111. Price R, Gustafson J, Greish K, Cappello J, McGill L, Ghandehari H. Comparison of silk-elastinlike protein polymer hydrogel and poloxamer in matrix-mediated gene delivery. International Journal of Pharmaceutics. 2012; 427:97–104. [PubMed: 21982738]

112. von Wald Cresce A, Dandu R, Burger A, Cappello J, Ghandehari H. Characterization and real-time imaging of gene expression of adenovirus embedded silk-elastinlike protein polymer hydrogels. Molecular Pharmaceutics. 2008; 5:891–897. [PubMed: 18763804]

113. Greish K, Araki K, Li D, O'Malley BW Jr, Dandu R, Frandsen J, Cappello J, Ghandehari H. Silk-elastinlike protein polymer hydrogels for localized adenoviral gene therapy of head and neck tumors. Biomacromolecules. 2009; 10:2183–2188. [PubMed: 19722557]

114. Greish K, Frandsen J, Scharff S, Gustafson J, Cappello J, Li D, O'Malley BW Jr, Ghandehari H. Silk-elastinlike protein polymers improve the efficacy of adenovirus thymidine kinase enzyme prodrug therapy of head and neck tumors. Journal of Gene Medicine. 2010; 12:572–579. [PubMed: 20603862]

115. Cappello J, Crissman JW, Crissman M, Ferrari FA, Textor G, Wallis O, Whitledge JR, Zhou X, Burman D, Aukerman L, Stedronsky ER. In-situ self-assembling protein polymer gel systems for administration, delivery, and release of drugs. Journal of Controlled Release. 1998; 53:105–117. [PubMed: 9741918]

116. Bayraktar O, Malay O, Ozgarip Y, Batigun A. Silk fibroin as a novel coating material for controlled release of theophylline. Eur J Pharm Biopharm. 2005; 60:373–381. [PubMed: 15996578]

117. Pritchard EM, Valentin T, Boison D, Kaplan DL. Incorporation of proteinase inhibitors into silkbased delivery devices for enhanced control of degradation and drug release. Biomaterials. 2010; 32:909–918. [PubMed: 20950854]

118. Cheema SK, Gobin AS, Rhea R, Lopez-Berestein G, Newman RA, Mathur AB. Silk fibroin mediated delivery of liposomal emodin to breast cancer cells. International Journal of Pharmaceutics. 2007; 341:221–229. [PubMed: 17499461]

119. Wang X, Zhang X, Castellot J, Herman I, Iafrati M, Kaplan DL. Controlled release from multilayer silk biomaterial coatings to modulate vascular cell responses. Biomaterials. 2008; 29:894–903. [PubMed: 18048096]

120. Wilz A, Pritchard EM, Li T, Lan JQ, Kaplan DL, Boison D. Silk polymer-based adenosine release: Therapeutic potential for epilepsy. Biomaterials. 2008; 29:3609–3616. [PubMed: 18514814]

121. You X, Chang JH, Ju BK, Pak JJ. Rapidly dissolving fibroin microneedles for transdermal drug delivery. Materials Science and Engineering C. 2011; 31:1632–1636.

122. Fang, JY.; Chen, JP.; Leu, YL.; Wang, HY. Chem Pharm Bull. Vol. 54. Tokyo: 2006. Characterization and evaluation of silk protein hydrogels for drug delivery; p. 156-162.

123. Gil ES, Panilaitis B, Bellas E, Kaplan DL. Functionalized Silk Biomaterials for Wound Healing. Advanced Healthcare Materials. 2013; 2:206–217. [PubMed: 23184644]

124. Zhang Y, Wu C, Luo T, Li S, Cheng X, Miron RJ. Synthesis and inflammatory response of a novel silk fibroin scaffold containing BMP7 adenovirus for bone regeneration. Bone. 2012; 51:704–713. [PubMed: 22796416]

125. Hofer M, Winter G, Myschik J. Recombinant spider silk particles for controlled delivery of protein drugs. Biomaterials. 2012; 33:1554–1562. [PubMed: 22079006]

126. Hofmann S, Foo CT, Rossetti F, Textor M, Vunjak-Novakovic G, Kaplan DL, Merkle HP, Meinel L. Silk fibroin as an organic polymer for controlled drug delivery. J Control Release. 2006; 111:219–227. [PubMed: 16458987]

127. Bessa PC, Balmayor ER, Azevedo HS, Nürnberger S, Casal M, Van Griensven M, Reis RL, Redl H. Silk fibroin microparticles as carriers for delivery of human recombinant BMPs. Physical characterization and drug release. Journal of Tissue Engineering and Regenerative Medicine. 2010; 4:349–355. [PubMed: 20058243]

128. Li C, Vepari C, Jin HJ, Kim HJ, Kaplan DL. Electrospun silk-BMP-2 scaffolds for bone tissue engineering. Biomaterials. 2006; 27:3115–3124. [PubMed: 16458961]

129. Schneider A, Wang XY, Kaplan DL, Garlick JA, Egles C. Biofunctionalized electrospun silk mats as a topical bioactive dressing for accelerated wound healing. Acta Biomaterialia. 2009; 5:2570–2578. [PubMed: 19162575]

130. Uebersax L, Mattotti M, Papaloizos M, Merkle HP, Gander B, Meinel L. Silk fibroin matrices for the controlled release of nerve growth factor (NGF). Biomaterials. 2007; 28:4449–4460. [PubMed: 17643485]

131. Madduri S, Papaloïzos M, Gander B. Trophically and topographically functionalized silk fibroin nerve conduits for guided peripheral nerve regeneration. Biomaterials. 2010; 31:2323–2334. [PubMed: 20004018]

132. Hopkins AM, De Laporte L, Tortelli F, Spedden E, Staii C, Atherton TJ, Hubbell JA, Kaplan DL. Silk hydrogels as soft substrates for neural tissue engineering. Advanced Functional Materials. 2013; 23:5140–5149.

133. Karageorgiou V, Meinel L, Hofmann S, Malhotra A, Volloch V, Kaplan D. Bone morphogenetic protein-2 decorated silk fibroin films induce osteogenic differentiation of human bone marrow stromal cells. Journal of Biomedical Materials Research - Part A. 2004; 71:528–537. [PubMed: 15478212]

134. Wang X, Kaplan DL. Functionalization of Silk Fibroin with NeutrAvidin and Biotin. Macromolecular Bioscience. 2011; 11:100–110. [PubMed: 20824692]

135. Yan HB, Zhang YQ, Ma YL, Zhou LX. Biosynthesis of insulin-silk fibroin nanoparticles conjugates and in vitro evaluation of a drug delivery system. Journal of Nanoparticle Research. 2009; 11:1937–1946.

136. Lin YC, Ramadan M, Hronik-Tupaj M, Kaplan DL, Philips BJ, Sivak W, Rubin JP, Marra KG. Spatially controlled delivery of neurotrophic factors in silk fibroin-based nerve conduits for peripheral nerve repair. Annals of Plastic Surgery. 2011; 67:147–155. [PubMed: 21712696]

137. Elia R, Newhide DR, Pedevillano PD, Reiss GR, Firpo MA, Hsu EW, Kaplan DL, Prestwich GD, Peattie RA. Silk-hyaluronan-based composite hydrogels: a novel, securable vehicle for drug delivery. J Biomater Appl. 2013; 27:749–762. [PubMed: 22090427]

138. Gu Y, Chen L, Yang HL, Luo ZP, Tang TS. Evaluation of an injectable silk fibroin enhanced calcium phosphate cement loaded with human recombinant bone morphogenetic protein-2 in ovine lumbar interbody fusion. Journal of Biomedical Materials Research - Part A. 2011; 97 A: 177–185. [PubMed: 21381189]

139. Wang X, Wenk E, Hu X, Castro GR, Meinel L, Li C, Merkle H, Kaplan DL. Silk coatings on PLGA and alginate microspheres for protein delivery. Biomaterials. 2007; 28:4161–4169. [PubMed: 17583788]

140. Mandal BB, Mann JK, Kundu SC. Silk fibroin/gelatin multilayered films as a model system for controlled drug release. European Journal of Pharmaceutical Sciences. 2009; 37:160–171. [PubMed: 19429423]

141. Mandal BB, Kapoor S, Kundu SC. Silk fibroin/polyacrylamide semi-interpenetrating network hydrogels for controlled drug release. Biomaterials. 2009; 30:2826–2836. [PubMed: 19203791]

142. Mandal BB, Kundu SC. Calcium alginate beads embedded in silk fibroin as 3D dual drug releasing scaffolds. Biomaterials. 2009; 30:5170–5177. [PubMed: 19552952]

143. Wenk E, Meinel AJ, Wildy S, Merkle HP, Meinel L. Microporous silk fibroin scaffolds embedding PLGA microparticles for controlled growth factor delivery in tissue engineering. Biomaterials. 2009; 30:2571–2581. [PubMed: 19157533]

144. Hines DJ, Kaplan DL. Mechanisms of controlled release from silk fibroin films. Biomacromolecules. 2011; 12:804–812. [PubMed: 21250666]

145. Lin CC, Metters AT. Hydrogels in controlled release formulations: Network design and mathematical modeling. Advanced Drug Delivery Reviews. 2006; 58:1379–1408. [PubMed: 17081649]

146. Peppas NA, Bures P, Leobandung W, Ichikawa H. Hydrogels in pharmaceutical formulations. European Journal of Pharmaceutics and Biopharmaceutics. 2000; 50:27–46. [PubMed: 10840191]

147. Siepmann J, Siepmann F. Mathematical modeling of drug delivery. International Journal of Pharmaceutics. 2008; 364:328–343. [PubMed: 18822362]

148. Peppas NA. Analysis of Fickian and non-Fickian drug release from polymers. Pharmaceutica Acta Helvetiae. 1985; 60:110–111. [PubMed: 4011621]

149. Ritger PL, Peppas NA. A simple equation for desciption of solute release I. Fickian and non-Fickian release from non-swellable devices in the form of slabs, spheres, cylinders or discs. Journal of Controlled Release. 1987; 5:23–36.

150. Ritger PL, Peppas NA. A simple equation for description of solute release II. Fickian and anomalous release from swellable devices. Journal of Controlled Release. 1987; 5:37–42.
151. Hines DJ, Kaplan DL. Characterization of small molecule controlled release from silk films. Macromolecular Chemistry and Physics. 2013; 214:280–294.
152. Wongpanit P, Ueda H, Tabata Y, Rujiravanit R. In vitro and in vivo release of basic fibroblast growth factor using a silk fibroin scaffold as delivery carrier. Journal of Biomaterials Science Polymer Edition. 2010; 21:1403–1419. [PubMed: 20534193]
153. Pritchard EM, Dennis PB, Omenetto F, Naik RR, Kaplan DL. Review: Physical and chemical aspects of stabilization of compounds in silk. Biopolymers. 2012; 97:479–498. [PubMed: 22270942]
154. Liebmann B, Hümmerich D, Scheibel T, Fehr M. Formulation of poorly water-soluble substances using self-assembling spider silk protein. Colloids and Surfaces A: Physicochemical and Engineering Aspects. 2008; 331:126–132.
155. Lu S, Wang X, Lu Q, Hu X, Uppal N, Omenetto FG, Kaplan DL. Stabilization of enzymes in silk films. Biomacromolecules. 2009; 10:1032–1042. [PubMed: 19323497]
156. Demura M, Asakura T, Kuroo T. Immobilization of biocatalysts with Bombyx mori silk fibroin by several kinds of physical treatment and its application to glucose sensors. Biosensors. 1989; 4:361–372.
157. Kuzuhara A, Asakura T, Tomoda R, Matsunaga T. Use of silk fibroin for enzyme membrane. Journal of Biotechnology. 1987; 5:199–207.
158. Liu Y, Zhang X, Liu H, Yu T, Deng J. Immobilization of glucose oxidase onto the blend membrane of poly(vinyl alcohol) and regenerated silk fibroin: Morphology and application to glucose biosensor. Journal of Biotechnology. 1996; 46:131–138.
159. Zhang YQ, Zhu J, Gu RA. Improved biosensor for glucose based on glucose oxidase-immobilized silk fibroin membrane. Applied Biochemistry and Biotechnology - Part A Enzyme Engineering and Biotechnology. 1998; 75:215–233.
160. Dennis PB, Walker AY, Dickerson MB, Kaplan DL, Naik RR. Stabilization of organophosphorus hydrolase by entrapment in silk fibroin: formation of a robust enzymatic material suitable for surface coatings. Biomacromolecules. 2012; 13:2037–2045. [PubMed: 22651251]
161. Lu Q, Wang X, Hu X, Cebe P, Omenetto F, Kaplan DL. Stabilization and release of enzymes from silk films. Macromol Biosci. 2010; 10:359–368. [PubMed: 20217856]
162. Panyam J, Labhasetwar V. Biodegradable nanoparticles for drug and gene delivery to cells and tissue. Advanced Drug Delivery Reviews. 2003; 55:329–347. [PubMed: 12628320]
163. Zhu G, Mallery SR, Schwendeman SP. Stabilization of proteins encapsulated in injectable poly (lactide-co- glycolide). Nature Biotechnology. 2000; 18:52–57.
164. Hu X, Kaplan D, Cebe P. Determining β-sheet Crystallinity in Fibrous Proteins by Thermal Analysis and Infrared Spectroscopy. Macromolecules. 2006; 39:6161–6170.
165. Motta A, Maniglio D, Migliaresi C, Kim HJ, Wan X, Hu X, Kaplan DL. Silk fibroin processing and thrombogenic responses. Journal of Biomaterials Science, Polymer Edition. 2009; 20:1875–1897. [PubMed: 19793445]
166. Takasu Y, Yamada H, Tsubouchi K. Extraction and chromatographic analysis of cocoon sericin of the silkworm. Bombyx mori, Journal of Insect Biotechnology and Sericology. 2002; 71:151–156.
167. Lammel A, Schwab M, Hofer M, Winter G, Scheibel T. Recombinant spider silk particles as drug delivery vehicles. Biomaterials. 2011; 32:2233–2240. [PubMed: 21186052]
168. PubMed Compound Database. [Accessed May 21, 2014] http://www.ncbi.nlm.nih.gov/pccompound.
169. Drug Bank. http://www.drugbank.ca/.

Article Highlights

- The structure and self-assembly mechanisms of silk are well characterized. Through this understanding, critical silk processing and formulation parameters can be identified for targeted pharmaceutical outcomes.
- Silk can be purified and processed into various biomaterial formats that are suitable for sustained drug delivery in aqueous-based solvents, avoiding toxic organics and aqueous-organic interfaces that may lead to drug instability.
- Silk is compatible with most common sterilization methods due to its high thermal stability and extraordinary mechanical properties. The possibility of terminal sterilization of silk formats could reduce manufacturing costs.
- Purified silk is a biocompatible material with low inflammatory, cytotoxic, and immunogenic potential. Impurities and contaminants on the native silk fibers that were the source of immunogenic responses in early reports are easily removable in aqueous solution.
- Long-term biocompatibility of various silk formats has been demonstrated in animal models lasting up to 1 year. This mirrors preclinical biological testing of the FDA-approved Seri® Surgical Scaffold (Allergan, Inc. MA), a silk-based biomaterial which demonstrated no toxicity, pyrogenicity, or allergenicity, as well as overall biocompatibility.
- Silk's predominantly hydrophobic, block copolymer structure and stimuli-responsive self-assembly pathway into β-sheet rich, supramolecular structures supports its robust mechanical properties and controllable, enzymatic biodegradation over days to months to years, depending on the degree of physical β-sheet crosslinking.
- Unlike most biopolymers, exceptionally strong physical interactions in silk enable its slow biodegradation rates without toxic chemical cross-linkers.
- Silk biodegradation is surface-mediated and presents opportunities for biodegradation-mediated, controlled drug release. This is in contrast with bulk hydrolysis of PLGA that results in continuous exposure of drugs to detrimental acidic microclimates.
- Unlike acidic byproducts of PLGA hydrolysis, silk biodegradation products are neutral amino acids that produce neither inflammatory reactions nor drug instability.
- The structural hierarchy of silk and its wide range of processing capabilities present effective network correlation lengths (pore sizes) from nanometer to micron-scale. This enables diffusion-controlled sustained delivery of bioactive molecules ranging from small molecules to genes to protein drugs.
- Drug diffusion kinetics in silk matrices can be further controlled by silk molecular weight, sequence modifications, and crystal structure/content to

manipulate silk-drug electrostatic and hydrophobic interactions, along with the hydration resistance and swelling behavior of the silk matrix.

- Injectable silk-based formulations, such as nano-/microsphere suspensions and hydrogels, have been used for the delivery of macromolecules of varied molecular weights including growth factors and monoclonal antibodies.
- For delivery of small molecules, silk-based implants such as films, coated tablets, reservoir systems, and 3D porous scaffolds have demonstrated the greatest control of sustained release rates.
- Recombinant silk analogs and silk-elastin-like copolymers are commonly used to deliver plasmid DNA or adenoviral vectors. Together with other beneficial properties of silk, the ability of these vehicles to be functionalized for targeted delivery offers an important advantage over other gene delivery systems.
- The high molecular weight of silk, along with its predominantly hydrophobic structure and versatile processing options enable its use as drug stabilization matrices in solution, semi-solid, and solid states. This has been demonstrated with small molecule and biological therapeutics including antibiotics, enzymes, vaccines, and monoclonal antibodies.
- An early development pathway to fibroin-based products is proposed outlining the critical need for well-characterized, robust, and scalable silk purification and processing methods combined with a systematic approach to formulation development, including careful selection of drug candidates, appropriate silk material formats, and manipulation of critical processing parameters to control pharmacokinetics.

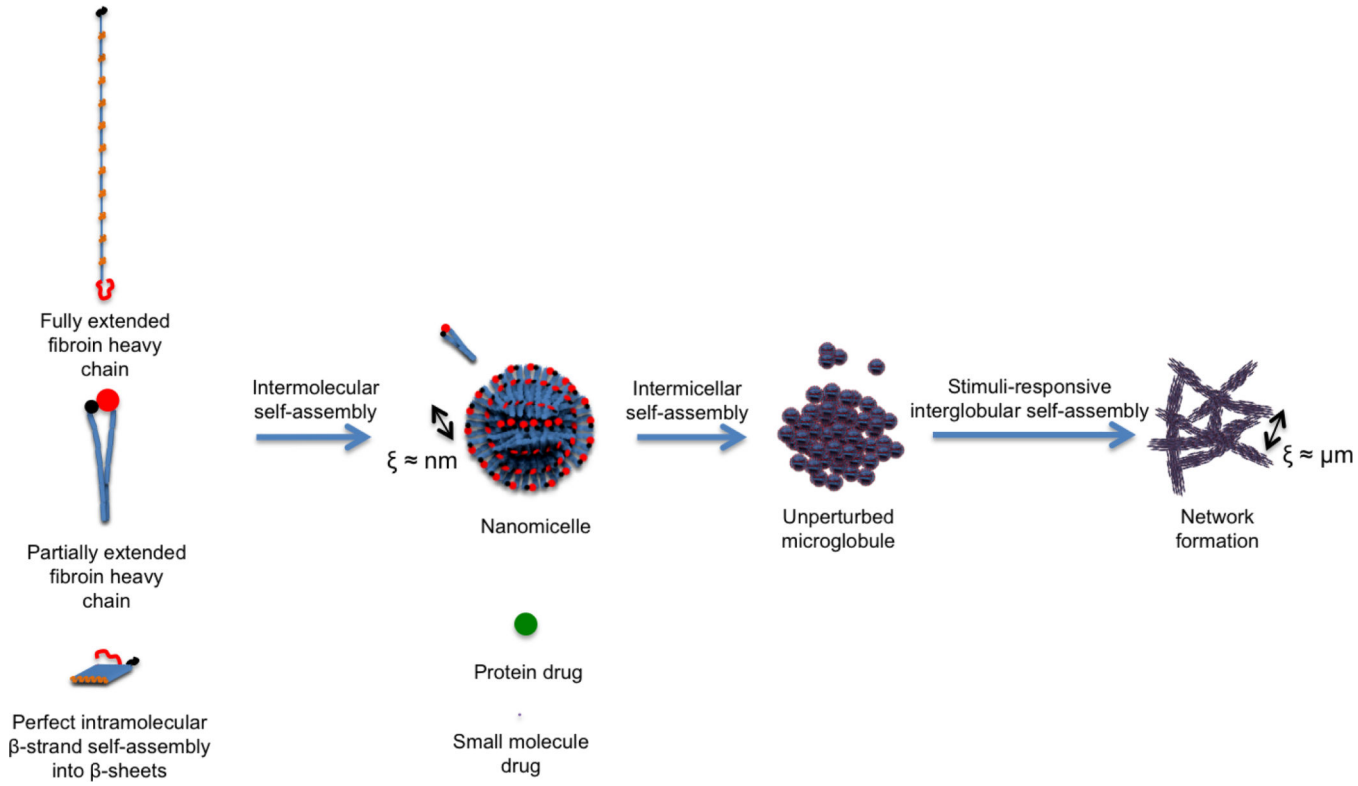

Figure 1.

The effective correlation lengths (ξ) in self-assembled silk fibroin structure for diffusion-controlled drug release (adapted from [51])

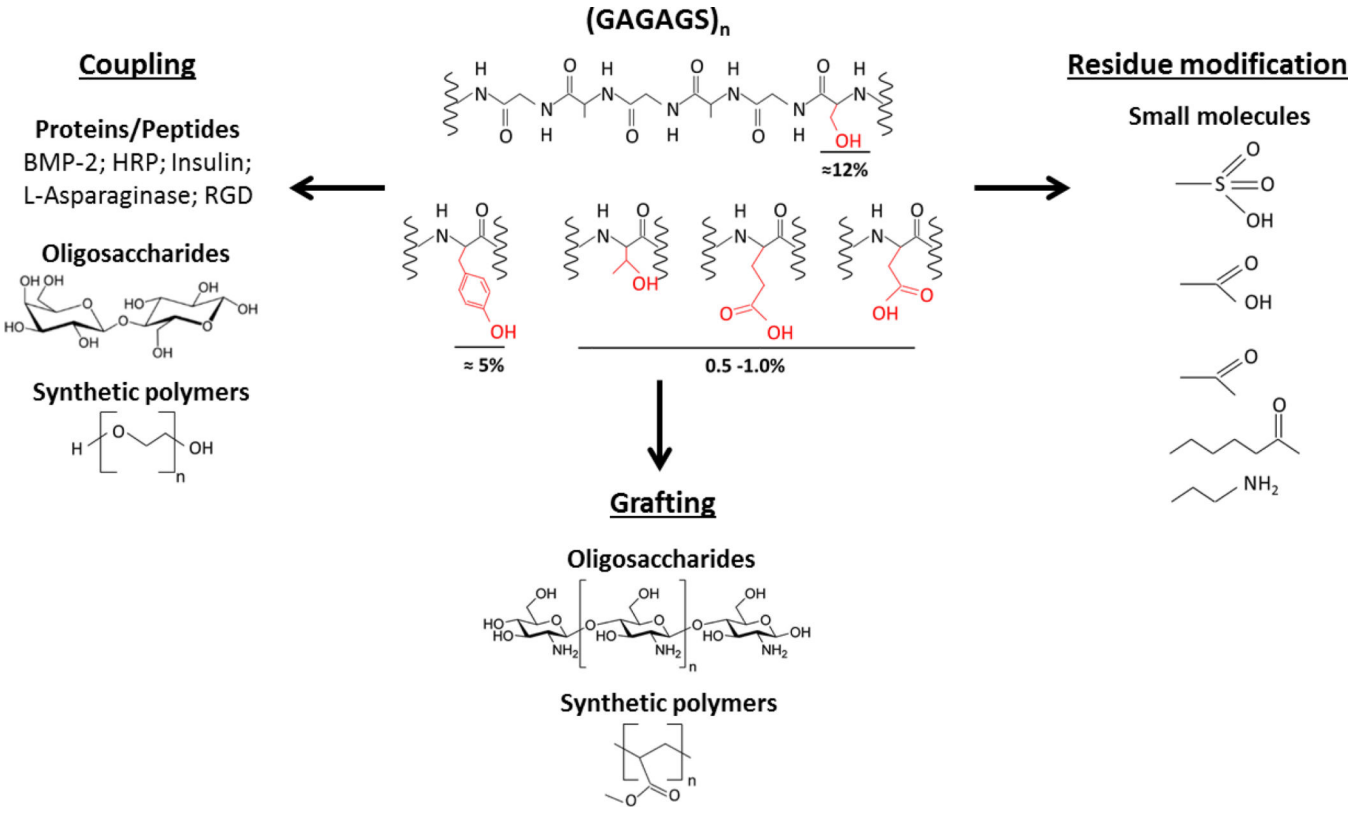

Figure 2.

Selected chemical modification approaches and molecules covalently bound to silk fibroin [42]. GAGAGS is the basic silk fibroin heavy chain repeat. The percentage values represent approximate molar density of reactive residues in silk fibroin heavy chain sequence. BMP-2: Bone Morphogenetic Protein, HRP: Horseradish Peroxidase, RGD: Arginylglycylaspartic acid.

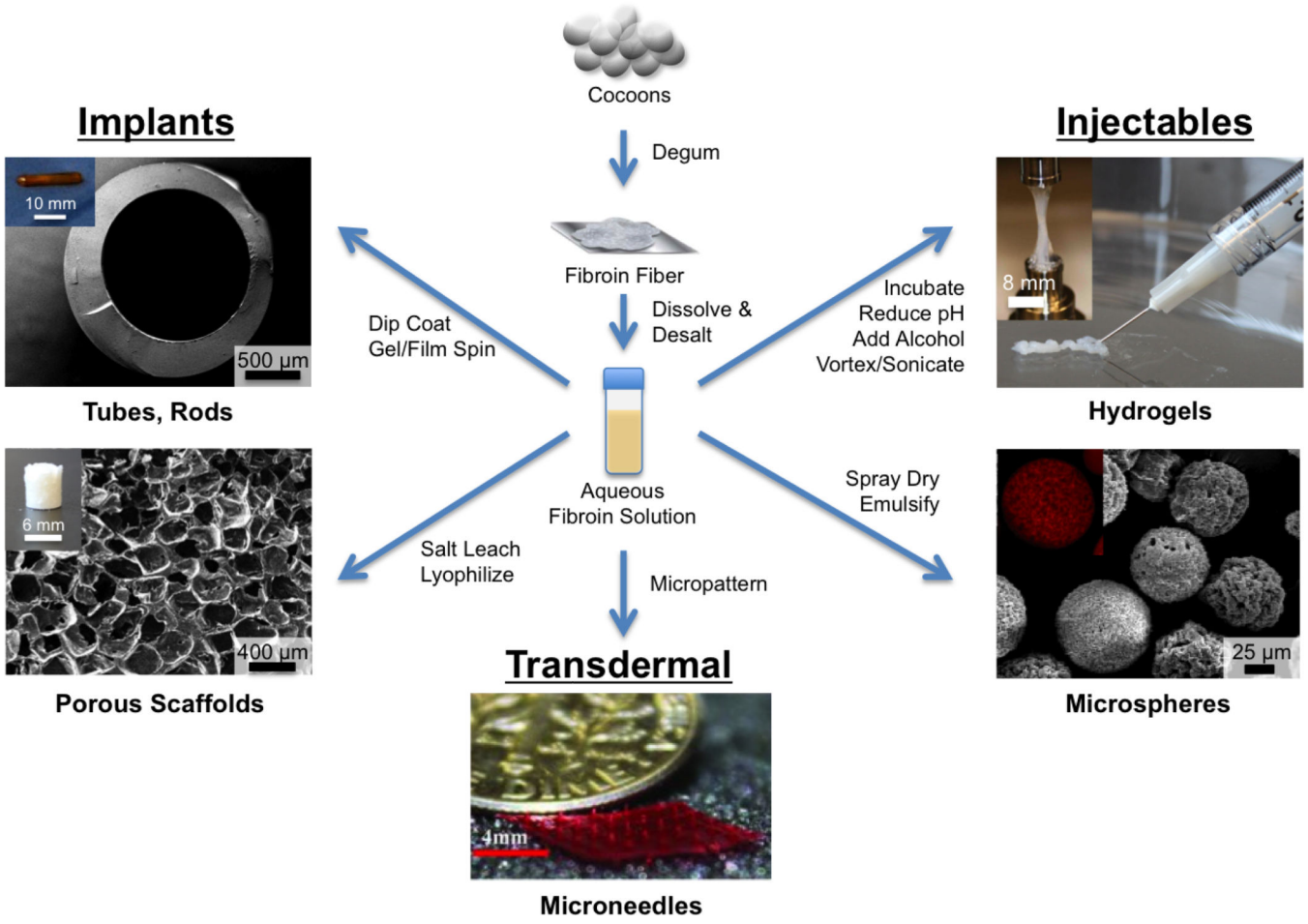

Figure 3.

Aqueous silk fibroin purification and example biomaterial processing options for sustained drug delivery. Transdermal microneedles image reprinted with permission from John Wiley & Sons, Inc. (Tsioris, et al. Advanced Functional Materials, 22 (2011) 330–335).

Table 1

The unique combination of desirable properties of silk for sustained drug delivery. Key distinctions versus synthetic polymer systems (e.g., PLGA) are highlighted in **bold**.

Structure	Predominantly hydrophobic, block copolymeric and modifiable sequence
	Self-assembly into β-sheet rich supramolecular structures
	Strong intra-/intermolecular physical interactions
	Stimuli-responsive crystal polymorphism
	High and tunable molecular weight
Processing	**Aqueous-based ambient purification and processing capabilities**
	Versatile material forms
	Suitability with common sterilization techniques
Physicochemical properties	Controllable network density, hydration resistance and swelling
	Controllable surface charge through sequence modifications
	High thermal stability
	Robust mechanical properties
	Tunable aqueous solubility
Biological properties	Low inflammatory/cytotoxic/immunogenic potential
	Enzymatic, surface mediated biodegradation
	Slow, controllable biodegradation rates
	Non-toxic, neutral biodegradation products (amino acids and peptides)
Pharmacological properties	Tunable release rates via diffusion- and biodegradation-controlled release
	Encapsulation of poorly soluble drugs
	Drug stabilization

Table 2

Key *in vivo* studies on silk fibroin biocompatibility and biodegradation

Silk Biomaterial	Model	Biocompatibility	Biodegradation	References
Films	Rat, I.M. implant	Less pronounced inflammatory reactions around fibroin than collagen or PLA	Not reported	[20]
Fibroin-RGD yarns	Rat, I.M. and S.C. implants; Goat, knee implant	No hypersensitivity reactions; Low immune responses to both silk and collagen controls	Complete biodegradation expected in 18 to 36 months	[12]
Porous scaffolds (6–10 wt% silk)	Rat, I.M. and S.C. implants	All scaffolds well tolerated; Mild, local and transient immune responses	Complete biodegradation in ≤6 months to ≥12 months depending on silk concentration, pore size, and interconnectivity	[15]
Ethanol induced hydrogels; Fibroin-RGD microgels (4–6 wt% silk)	Rat, S.C implant; Guinea pig, I.D. injection	23-RGD modification improved fibroin biocompatibility; Similar host response to fibroin-RGD and collagen controls	Similar biodegradation of fibroin-RGD and collagen controls; 75% of all sites had residual material after 92 days	[17]
Acidic hydrogels (2 wt% silk)	Rabbit, knee implant	No inflammatory reactions; Fibroin hydrogels promoted bone remodeling	Partial biodegradation in 12 weeks	[18]
Sonicated hydrogels (1–2 wt%)	Rat, knee implant	Not reported	Complete biodegradation in 12 weeks	[11]

I.M. = Intramuscular; S.C. = Subcutaneous; I.D. = Intradermal

Table 3

Silk-based formulation approaches for sustained delivery of genes

Formulation	Gene Delivery	Construct Size (kbp)	Sustained Release Duration (days)	References
Spider silk consensus repeat/poly(L-lysine) ionic complexes	Plasmid DNA			
	pDNA-GFP	7.65	----	[43. 105]
	pDNA-Luc	7.04	----	[95, 104, 105]
Silk-elastin-like polymer hydrogels	pDNA (pUC18)	2.60	28[1]	[92]
	pDNA (pRL-CMV)	4.08	28[1] 28[2]	[92]
	pDNA (pRL-CMV-Luc)	4.08	28[1]	[107]
	pDNA (pCFB-EGSH-Luc)	8.50	28[1]	[92]
	pDNA (pFB-ERV)	11.0	28[1]	[92]
	Adenovirus			
	Ad-CMV-GFP		28[1]	[92]
	Ad-GFP		28[1] 28[2]	[110]
	Ad-CMV-LacZ		28[1] 21[2]	[108, 110, 113]
	Ad-CMV-Luc		15–21[2]	[108, 112, 113]
	Ad-Luc-HSVtk		28–50[2]	[109,111]
	Ad-Tk		14[2]	[113]
	Ad-Luc-Tk		33[2]	[114]
3D porous scaffold	Ad-BMP7		21[1]	[124]

pDNA = Plasmid DNA; Ad = Adenovirus; GFP = green fluorescent protein; Luc = luciferase reporter gene; CMV = cytomegalovirus promoter gene; LacZ = beta galactosidase reporter gene; HSVtk = herpes simplex virus thymidine kinase gene; Tk = thymidine kinase gene; BMP7 = bone morphogenic protein 7;

[1] = *in vitro* release data;

[2] = *in vivo* release data

Table 4

Silk-based formulation approaches for sustained delivery of small molecule drugs

Formulation	Small Molecule Drug	Molecular Weight (Da)	pKa [168,169]	logP [168,169]	Sustained Release Duration (days)	References
Implants						
Tablets	Theophylline	180	8.8	0.0	<1[1]	[116]
	Adenosine	267	3.6, 12.4	−1.1	10–17[1]	[96, 117]
Films/coatings	Penicillin	356	2.8	1.8	1[1]	[99]
	Ampicillin	371	2.5, 7.3	1.4	1[1]	[99]
	Clopidogrel	420	5.3	3.8	28[1]	[119]
	Cefazolin	455	3.6	−0.6	3[1]	[99]
	Indigo carmine	466			14[1]	[91]
	Gentamicin	478		−3.1	5[1]	[99]
	Rhodamine B	479			35[1]	[98]
	Rifampicin	823	1.7	4.2	3–14[1]	[91, 99]
	Paclitaxel	854		3.0	28[1]	[119]
	Reactive red 120	1470			7[1]	[91]
3D porous scaffolds (+/− microspheres)	Adenosine	267	3.6, 12.4	−1.1	14[1] 20[2]	[120]
	Erythromycin	734	8.9	3.1	31[1]	[99]
	Rifampicin	823	1.7	4.2	9[1]	[99]
Injectables						
Microcapsules	Emodin	270			4–6[1]	[97, 118]
Microspheres/nanospheres	Salicylic acid	138	3.0, 13.6	2.3	1[1]	[34]
	Propranolol HCl	296	9.5	−0.5	28[1]	[34]

Formulation	Small Molecule Drug	Molecular Weight (Da)	pKa [168,169]	logP [168,169]	Sustained Release Duration (days)	References
	Rhodamine B	479			14[1]	[33]
Hydrogels (silk-only or composites, +/− microspheres)	Penicillin	356	2.8	1.8	2–4[1]	[99]
	Prednisone	358		1.5	<1[1]	[137]
	Prednisolone	360		1.6	<1[1]	[137]
	Cortisone	360			<1[1]	[137]
	Hydrocortisone	363		1.6	1–2[1]	[137]
	Ampicillin	371	2.5, 7.3	1.4	3–4[1] 1[2]	[99]
	6α-methylprednisolone	375		1.8	2[1]	[137]
	Dexamethasone	393		1.8	2[1]	[137]
	Buprenorphine HCl	504	8.3	5.0	<1[1]	[122]
Transdermal						
Microneedles	Tetracycline	444	3.3	−1.4	<1[1]	[73]

[1] = *in vitro* data;

[2] = *in vivo* data

Table 5

Silk-based formulation approaches for sustained delivery of biological drugs

Formulation	Biological Drug	Molecular Weight (kDa)	Sustained Release Duration (days)	References
Implants				
Films/coatings (silk-only or composites)	Inulin	3.9	28[1]	[140]
	Dextran	4–40	28[1]	[126]
	EGF	6	12[2]	[123]
	NGF	13.5	22[1]	[130]
	Lysozyme	14.3	23[1]	[126]
	Heparin	15	28[1]	[119]
	FGF-2	17	6[1]	[44]
	HRP	44	23[1]	[126]
	BSA	66	28[1]	[140]
	Azoalbumin	66.4	30–35[1]	[91, 98]
Electrospun fibers/mats/tubes/scaffolds	EGF	6	7[1], 12[2]	[123, 129]
	NGF	13.5	28[1]	[131]
	GDNF	15	28[1]	[131]
	BMP-2	26	Not reported	[128]
Tubes/conduits (+/− microspheres)	NGF	13.5	22[1]	[130]
	GDNF	15	≈42[2]	[136]
3D porous scaffolds (silk-only or composites, +/− microspheres)	Inulin	3.9	35	[142]
	IGF-1	7.6	29–49[1]	[101, 103, 143]
	BMP-2	26	≈7–35[1], ≈14–28[2]	[100, 103]
	BSA	66	35[1]	[142]
Lyogels	Anti-TGFβ IgG1	150	38–160[1]	[41, 102]
Injectables				
Bioconjugate solutions	Insulin	5.8	≈2[1], ≈1[2]	[45]
Microspheres/nanospheres (silk-only or composite)	Insulin	5.8	<<1[1]	[135]
	IGF-1	7.6	14–49[1]	[34, 103]
	Dextran	10	14[1]	[33]
	Lysozyme	14.3	28[1]	[125]
	BMP-(2,9,14)	24–27	14[1]	[103, 127]
	HRP	44	15–32[1]	[32, 139]

Formulation	Biological Drug	Molecular Weight (kDa)	Sustained Release Duration (days)	References
	BSA	66	14–16[1]	[33, 139]
Hydrogels (silk-only or composites)	Inulin	3.9	45[1]	[141]
	Dextran	4–250	1–4[1]	[137]
	NT-3	27.2	25[1]	[132]
	VEGF	38.2	42[1]	[137]
	Anti-TGFβ IgG1	150	26[1]	[102]
Transdermal				
Microneedles	HRP	44	2[1]	[73]

EGF = epidermal growth factor; NGF = nerve growth factor; FGF = fibroblast growth factor; HRP = horseradish peroxidase; BSA = bovine serum albumin; GDNF = glial cell line-derived neurotrophic factor; BMP = bone morphogenic protein; IGF = insulin-like growth factor; NT-3 = neurotrophin-3; VEGF = vascular endothelial growth factor;

[1] = *in vitro* data;

[2] = *in vivo* data

Table 6

Proposed mechanisms of drug stabilization in silk based formulations

	Sources of Instability	Proposed Stabilization Mechanism	References
Small Molecule Drugs	Poor water solubility Inactivity in aqueous media	Hydrophobic interactions Amphiphilicity of silk fibroin	[99, 154]
Biological Drugs	Aggregation/denaturation Thermal instability pH inactivation Enzymatic degradation	Hydrophilic/hydrophobic interactions Immobilization/sequestration in silk matrix Reduced molecular mobility Structural stabilization Reduced moisture content	[31, 153, 155, 161]